Section 3 Optics and Devices

Chapter 1. Optics and Quantum Electronics

Academic and Research Staff

Professor Hermann A. Haus, Professor Erich P. Ippen, Professor James G. Fujimoto, Professor Peter L. Hagelstein, Dr. Santanu Basu, Dr. Joseph A. Izatt

Visiting Scientists and Research Affiliates

Dr. Lucio H. Acioli, Dr. Guiseppe Gabetta, Dr. Yuzo Hirayama, Dr. Franz X. Kärtner, Dr. Charles P. Lin, Dr. Antonio Mecozzi, Dr. Kazunori Naganuma, Dr. Masataka Shirasaki

Graduate Students

Keren Bergman, John Paul Braud, Jerry C. Chen, Isaac L. Chuang, Jay N. Damask, Christopher R. Doerr, David J. Dougherty, James G. Goodberlet, Katherine L. Hall, Michael R. Hee, David Huang, Charles T. Hultgren, Janice M. Huxley, Sumanth Kaushik, Farzana I. Khatri, Joseph M. Jacobson, Yinchieh Lai, Gadi Lenz, John D. Moores, Ann W. Morgenthaler, Martin H. Muendel, Lynn E. Nelson, Janet L. Pan, Malini Ramaswamy, Kohichi R. Tamura, Morrison Ulman

Undergraduate Students

Michele M. Bierbaum, Irfan U. Chaudhary, Stephen Y. Hon

Technical and Support Staff

Mary C. Aldridge, Donna L. Gale, Cynthia Y. Kopf, Lisbeth N. Lauritzen

1.1 Additive Pulse Modelocking

Sponsors

Joint Services Electronics Program
Contract DAAL03-89-C-0001
Contract DAAL03-92-C-0001
U.S. Air Force - Office of Scientific Research
Contract F49620-91-C-0091

Project Staff

Professor Hermann A. Haus, Professor Erich P. Ippen, Dr. Antonio Mecozzi, Jerry C. Chen, Farzana I. Khatri, John D. Moores, Stephen Y. Hon

Additive Pulse Modelocking (APM) is a technique of mode locking that simulates a fast saturable absorber via nonlinear interferometric action using a Kerr medium. Often this medium is a fiber placed in an auxiliary cavity, but the Kerr effect may be produced in the components internal to the main cavity of the laser. The Kerr Lens Modelocking pioneered by Coherent, produces equivalent saturable absorber action by self focusing. A general theory has been developed for both kinds of systems.[1] Its main results are:

1. An analytic treatment of the modelocking process in the presence of self-phase modulation and group velocity dispersion;
2. Criteria for the stability of the modelocked pulses;
3. The condition for self starting of the pulses and the explanation of a power threshold for mode locking.[2]

The theory is helpful in pointing the way to the generation of shorter pulses with lower fluctuations.

In conjunction with this theory, an analysis of noise in modelocked systems has been carried out.[3] This analysis provides an explanation of the observed spectra of the detector current illumi-

1 H.A. Haus, J.G. Fujimoto, and E.P. Ippen, "Structures for Additive Pulse Modelocking," *J. Opt. Soc. Am. B* 8: 2068-2076 (1991).

2 H.A. Haus and E.P. Ippen, "Self Starting of Passively Modelocked Lasers," *Opt. Lett.* 16: 1331-1333 (1991).

3 S. Hon, K. Bergman, A. Mecozzi, and H.A. Haus, "Noise Spectra of Modelocked Laser Pulses," submitted for presentation at CLEO '92, Anaheim, CA (1992).

nated by modelocked pulses observed by many researchers. Stephen Hon has performed extensive measurements of three different laser systems (actively modelocked Nd:YAG, soliton laser, APM Ti:Sapphire laser). We have shown theoretically that the current spectrum reveals not only the amplitude and timing jitter, as heretofore assumed, but also gives information on the correlation between the two. These experiments have been an important guide to the theory. Conversely, the newly developed theory is now being applied to extract full information from the detector current spectra. The fluctuations that are not observable from the current spectrum of direct detection are the phase fluctuations (that give rise to the well-known Schawlow-Townes linewidth) and the carrier frequency fluctuations.

The analysis has also been extended to allow for the inclusion of slow, as well as fast, absorber effects. Such a combination may be used to advantage in lasers where pulse initiation is a problem. There is a trade-off in the range of gain and dispersion over which steady-state stability can be achieved.

1.2 Ultrashort Pulse Fiber Laser

Sponsors

Charles S. Draper Laboratories
 Contract DL-H-441629
Joint Services Electronics Program
 Contract DAAL03-89-C-0001
 Contract DAAL03-92-C-0001
U.S. Air Force - Office of Scientific Research
 Contract F49620-91-C-0091

Project Staff

Professor Hermann A. Haus, Professor Erich P. Ippen, Janice M. Huxley, Lynn E. Nelson, Kohichi R. Tamura

High bit-rate optical communication networks and ultrafast optical signal processing systems will require compact, chirp-free picosecond pulse sources. Erbium-doped fiber lasers are prime candidates because of their compatibility with transmission fibers, their operation at 1.5 μm, and their amenability to diode pumping. The nonlinear refractive index effects in these fibers also make them attractive lasers for additive pulse mode-locking (APM). We have therefore constructed an erbium fiber laser with intent to study how APM may be implemented in an all-fiber device and to optimize ultrashort pulse generation.

In a fiber, the nonlinear interferometric action necessary for APM is most easily achieved through intensity dependent polarization rotation. Thus our laser uses fiber polarizers and polarization controllers in a fiber ring with an erbium amplifying section. Fiber couplers to the ring facilitate pumping (with a Ti:sapphire laser for the time being) and output coupling. Short pulse operation has already been obtained and studied under several operating conditions. Pulse spectra indicate durations as short as 300 fs. Autocorrelation measurements and variations with pumping level indicate that the output consists of strings of pulses quantized by soliton effects. A computer model has been developed that extends our APM theory to cases like this in which pulse shaping effects per round trip are large and cannot be treated perturbationally. This model is now being used to map regions of stability and single pulse operation.

1.3 Long Distance Fiber Communications

Sponsor

MIT Lincoln Laboratory

Project Staff

Professor Hermann A. Haus, Dr. Antonio Mecozzi, Yinchieh Lai, John D. Moores

In 1986, J.P. Gordon and Professor Hermann A. Haus published a paper[4] pointing out that transatlantic transmission using solitons would suffer from timing jitter of the pulses caused by frequency jitter induced by the spontaneous emission of the amplifier stages. This effect, now called the Gordon-Haus effect, has had an important influence on the planning of the next transatlantic cable of AT&T which will be laid in 1995. This cable will not use solitons, but will operate at (or near) the zero dispersion wavelength of the fiber. It is designed for 5 Gbit transmission and so that future Wavelength Division Multiplexing will not be permitted, at least not when using similar channels shifted in frequency. The reason for this design is that the dynamic range of the input pulse stream of the soliton version of the system is limited by two effects. On one hand, the pulses have to be energetic enough

[4] J.P. Gordon and H.A. Haus, "Random Walk of Coherently Amplified Solitons in Optical Fiber Transmission," *Opt. Lett.* 11: 665-667 (1986).

to overcome detector shot noise. On the other hand, if too powerful, the Gordon-Haus effect produces excessive timing jitter.

We have come up with a means of combatting the Gordon-Haus effect using periodically spaced filters.[5] Kodama and Hasegawa at AT&T Bell Laboratories have proposed this scheme independently, and Mollenhauer has tested it. Because the information was company confidential, we were not aware of it until recently. As of this date (12/19/91), their paper had not been published. The scheme permits wavelength multiplexing because the filter to be used could be a Fabry-Perot with a characteristic period in frequency.

1.4 Squeezing

Sponsors

Charles S. Draper Laboratories, Inc.
Contract DL-H-418478
Fujitsu Laboratories
National Science Foundation
Grant ECS 90-12787

Project Staff

Professor Hermann A. Haus, Keren Bergman, Christopher R. Doerr, Dr. Masataka Shirasaki, Dr. Franz X. Kärtner

The successful squeezing experiments of last year have been continued. It should be reemphasized that our squeezing scheme in a fiber ring[6] can save, in principle, all the pump power for local oscillator power, and hence is superior to schemes that "waste" the pump (such as those using parametric amplification).

Figure 1 shows the experimental setup that has been used to observe both reduced and increased shot noise as a function of phase between local oscillator (derived from the pulse used for squeezing) and the squeezed radiation. The upper trace in figure 2 shows the calibrated shot noise level, the lower trace shows the noise as a function of mirror position that changes the phase between the L.O. and the squeezed light. The center frequency is 40 kHz, the bandwidth is 2 kHz. Although this may not be the best way to determine the degree of squeezing (5 dB below shot noise), it is a rather spectacular display of squeezing and antisqueezing.

We have measured the noise of the laser oscillator (part of the motivation for the study of mode-locked laser noise described above was motivated by this investigation) and found that the mode locked Nd:YAG laser produces noise only 20 dB above shot noise at frequencies of 40 kHz and higher (and away from the line spectrum of pulse repetition periodicity). Our balanced detector is designed to suppress 30 dB or more of the local oscillator noise.

We have also initiated a thorough study of the Guided Acoustic Wave (GAWBs) noise observed by the IBM group. We have found that the contributions of GAWBS are not large enough to have affected our noise spectra in the low frequency regime (40-80 kHz).

We have succeeded in stabilizing the phase between the local oscillator and the squeezed radiation to achieve a constant noise reduction of 5 dB below shot noise. In a future experiment, this system will be employed to demonstrate sub shot noise interferometric detection in a future experiment.

We envisage that squeezing will eventually be used in fiber gyros that would operate below the shot noise level. We have studied the problem of the nonlinearity of the Sagnac fiber and found that, to take advantage of the squeezed radiation noise reduction, the Sagnac loop must have reduced nonlinearity.[7]

1.5 Integrated Optics Components

Sponsors

National Science Foundation
Grant ECS 90-12787
National Center for Integrated Photonics

---

5 A. Mecozzi, J.D. Moores, H.A. Haus, and Y. Lai, "Soliton Transmission Control," *Opt. Lett.* 16: 1841-1843 (1991).

6 M. Shirasaki and H.A. Haus, "Squeezing of Pulses in a Nonlinear Interferometer," *J. Opt. Soc. Am. B* 7: 30-34 (1990).

7 H.A. Haus, K. Bergman, and Y. Lai, "Fiber Gyro With Squeezed Radiation," *J. Opt. Soc. Am. B* 8: 1952-1957 (1991).

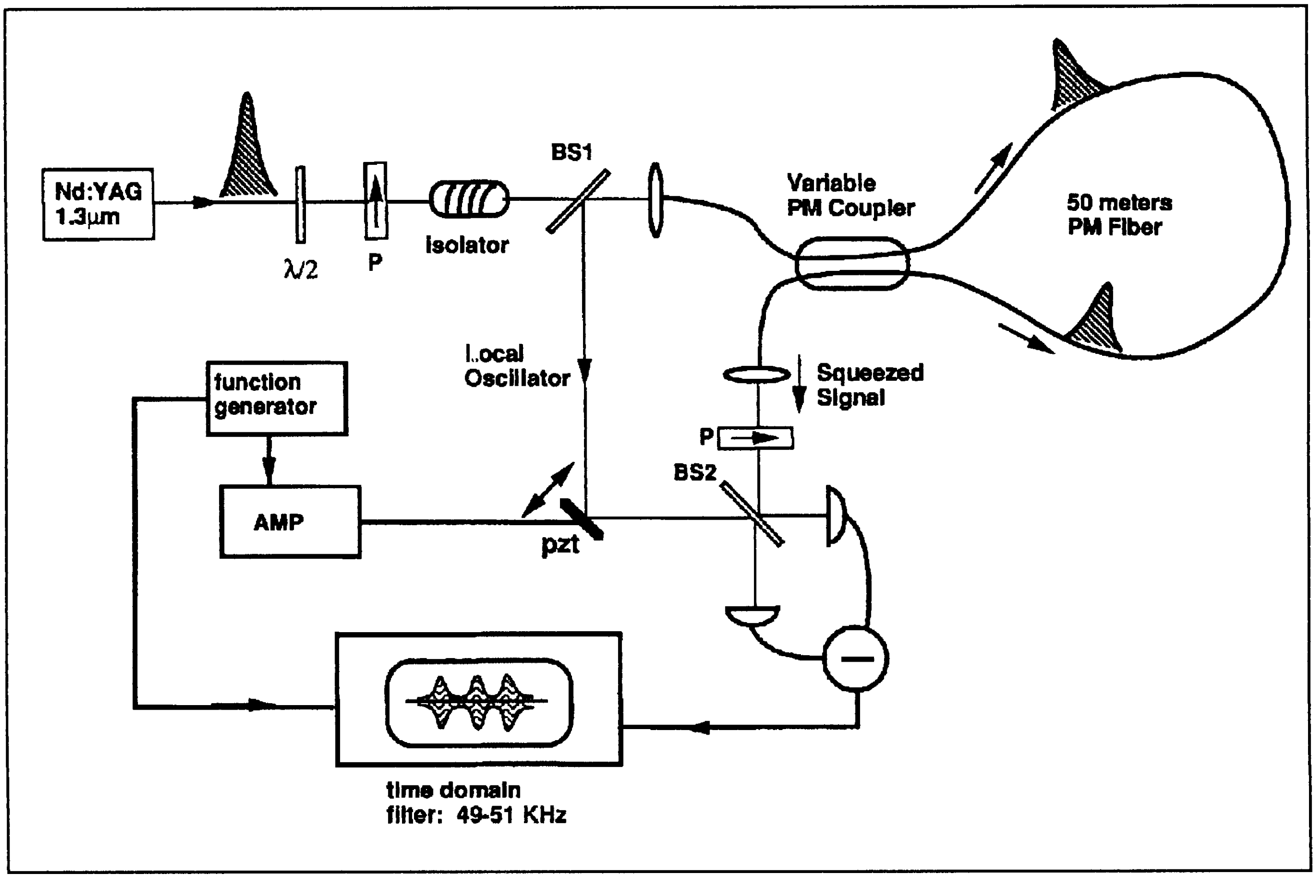

Figure 1.

Project Staff

Professor Hermann A. Haus, Jay N. Damask, Professor Henry I. Smith, Vincent V. Wong

Fiber communications using wavelength division multiplexing requires channel dropping filters to avoid the power loss due to "broadcasting" of all channels. No proposal existed for a cascadable channel dropping filter that would be narrow-band enough to accommodate channels of bandwidth corresponding to Gbit transmission rates. We have proposed a channel dropping filter of a new design,[8] based on the quarter wave shifted Distributed Feedback Structure patented by H.A. Haus and C.V Shank in 1976. The structure is already in wide use for frequency stable DFB lasers. In this novel application, the structure is side-coupled to the "transmission bus" to affect only the channel to be dropped. Various forms of the design have been laid out, one of which employs an active layer for amplification and reinjects the dropped signal so that it can be detected "downstream." We have begun the fabrication of a prototype device in collaboration with Professor Henry I. Smith of the MIT Submicron Structures Laboratory. In conjunction with the tuning scheme pursued in collaboration with Professor Clifton G. Fonstad described below, the channel dropping filters could be made tunable.

1.6 Tunable Lasers

Sponsor

National Center for Integrated Photonics

Project Staff

Professor Hermann A. Haus, Professor Clifton G. Fonstad, Paul S. Martin

Tunable lasers have been constructed successfully with Bragg Reflectors whose optical index is changed by current injection. The laser section of the structure itself is maintained at constant gain

[8] H.A. Haus and Y. Lai, "Narrow-band Optical Channel Dropping Filter," *IEEE J. Lightwave Technol.* 10: 57-62 (1992).

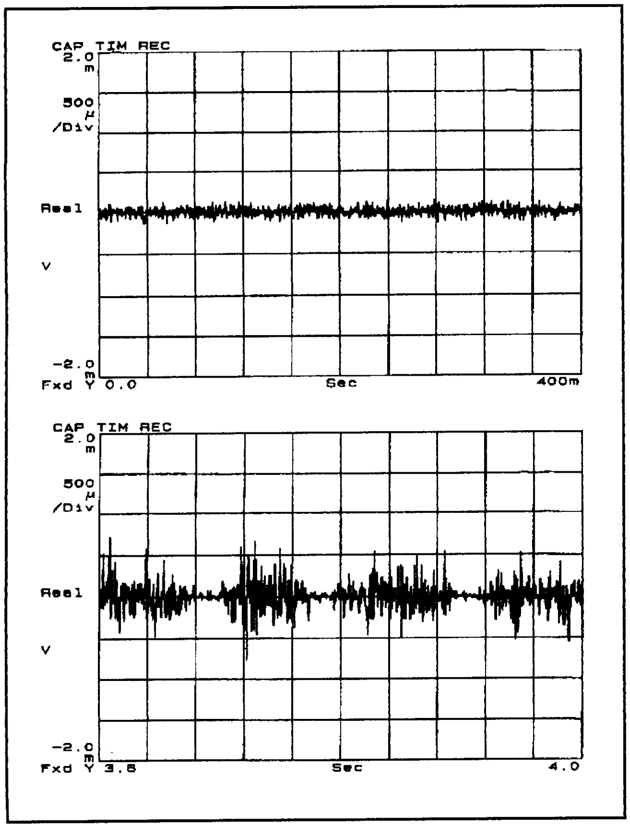

Figure 2.

by keeping its injection current relatively constant. Such structures have achieved wide tuning ranges, but not in a continuous manner.

We are pursuing an alternate approach that relies on the ability of controlling the injection currents into two quantum wells, one on top of the other, by contacts properly fabricated by ion implantation. The two quantum wells are different and have transitions at different frequencies. The respective gain peaks are displaced in frequency, and, along with them, the index characteristics. By controlling the currents injected into the two quantum wells separately, one can control the gain and index independently. Such structures would be ideal for tuning of monolythic resonators at constant gain.

1.7 Gain Dynamics in Semiconductor Amplifiers

Sponsors

Joint Services Electronics Program
Contract DAAL03-89-C-0001
Contract DAAL03-92-C-0001
National Science Foundation
Grant EET 88-15834
U.S. Air Force - Office of Scientific Research
Contract F49620-91-C-0091

Project Staff

Professor Erich P. Ippen, Katherine L. Hall, Gadi Lenz, Dr. Kazunori Naganuma

The potential application of semiconductor amplifiers to wideband communication networks and integrated photonic circuits motivates our studies of these devices. We use femtosecond optical pulses to probe propagation effects in amplifier structures, characterize optical nonlinearities in the gain, and observe fundamental ultrafast carrier dynamics in the semiconductor active layers.

During the past year we have performed the first femtosecond time-domain measurements of group velocity dispersion (GVD) in diode lasers at 1.5 μm.[9] The effects of GVD are two-fold: (1) it can distort pulses being transmitted and amplified, and (2) it limits the temporal resolution, or frequency bandwidth, of nonlinear optical interactions. Our measurements, in both bulk and multiple-quantum-well (MQW) samples yield values for $\lambda d^2 n_{eff}/d\lambda^2$ in the range -0.63 to 0.95 μm^{-1} and indicate that intrinsic material dispersion is the dominant factor. In addition, we discovered differences in group velocity between TE and TM modes on the order of 200 fs/mm. These must be accounted for in studies of anisotropic nonlinearities.

We have also demonstrated a new technique for femtosecond pump-probe measurement that makes it possible to use parallel-polarized pump and probe beams even in strictly collinear geometries.[10] The method makes use of acousto-optic frequency shifting and relies on heterodyne detection to distinguish between pump and probe pulses. In experiments with bulk (V-groove) diode amplifiers, we have demonstrated the obser-

9 K.L. Hall, G. Lenz, and E.P Ippen, "Femtosecond Time Domain Measurements of Group Velocity Dispersion in Diode Lasers at 1.5 μm," *J. Lightwave Tech.*, forthcoming, May 1992.

10 K.L. Hall, G. Lenz, E.P. Ippen, and G. Raybon, "Heterodyne Pump-Probe Technique for Time-Domain Studies of Optical Nonlinearities in Waveguides," submitted to *Opt. Lett.*

vation of differences due to nonlinear as well as linear anisotropy. Preliminary results have been obtained on strained-layer quantum-well devices which have highly anisotropic gain.

1.8 Ultrafast Optical Kerr Effect in Active Waveguides

Sponsors

National Center for Integrated Photonics
National Science Foundation
  Grant EET 88-15834
U.S. Air Force - Office of Scientific Research
  Contract F49620-91-C-0091

Project Staff

Professor Erich P. Ippen, David J. Dougherty, Charles T. Hultgren

Active optical waveguides offer interesting possibilities for performing nonlinear functions in photonic circuits. By varying the injected carrier density one can change not only the linear components of gain and index of refraction but also the nonlinear ones. A particularly interesting regime of operation is that near the point of nonlinear transparency. At that point, an optical pulse traveling through the waveguide neither creates carriers by absorption nor removes carriers by stimulated emission. There is no long-lived change. Yet the optical wavelength is above bandgap and the density of carriers in the medium is high.

In previous studies of gain dynamics in AlGaAs lasers near this point, we discovered a large transient gain nonlinearity which we identified with nonequilibrium carrier heating. The initial purpose of the work described here was to investigate the index of refraction dynamic associated with this gain nonlinearity. We have done so,[11] using a time-division interferometric technique originally demonstrated by Professor Fujimoto's group in passive guides. With this technique we have observed the predicted index dynamic in channeled-substrate planar (CSP) AlGaAs diode lasers (Hitachi HLP 1400) biased just below threshold. The dynamic is identified by its approximately 1.7 ps recovery time and positive sign that is consistent with a theoretical calculation for nonequilibrium heating. To our surprise, however, these experiments have also uncovered a faster and even larger index change. We attribute this new component to an above-band optical Stark shift.[12]

Our experiments were performed with orthogonally polarized pump and probe, so that what we measure is $n_{2\perp}$. The ultrafast Stark-like component has a negative sign, as do below-bandgap values, but an enhanced value of about $-5 \times 10^{-12} cm^2/W$. We believe that the resonant enhancement in the active region has contributions from filled states below the laser photon energy as well as from filled states above. A theoretical description of this possibility has now been put forward by Sheik-Bahai.[13] Such an effect may have application to ultrafast optical switching. It can also provide a new means for studying femtosecond carrier relaxation phenomena in semiconductors.

1.9 Coherent Phonons in Electronic Materials

Sponsors

Joint Services Electronics Program
  Contract DAAL03-89-C-0001
  Contract DAAL03-92-C-0001
U.S. Air Force - Office of Scientific Research
  Contract F49620-91-C-0091

Project Staff

Professor Erich P. Ippen, Tak K. Cheng, Siegfried B. Fleischer

With optical pulses shorter than 100 fs it has become possible to excite and observe in the time domain the coherent oscillation of optical phonons with frequencies up to 10 THz (333 cm^{-1}). In collaboration with Professor Dresselhaus' group we have been investigating the application of this possibility to electronic materials. Recently, we have reported that excitation of such phonons is

[11] C.T. Hultgren and E.P. Ippen, "Ultrafast Refractive Index Dynamics in AlGaAs Diode Laser Amplifiers," *Appl. Phys. Lett.* 59: 635 (1991).

[12] C.T. Hultgren and E.P. Ippen, "Ultrafast Optical Kerr Effect in Active Semiconductor Waveguides," *Proceedings of the O.S.A. Topical Meeting on Nonlinear Guided-Wave Phenomena,* paper TuB2, Cambridge, England, September 1991.

[13] M. Sheik-Bahai and E.W. Van Stryland, "Theory of Ultrafast Nonlinear Refraction in Semiconductor Lasers," *Proceedings of the O.S.A. Annual Meeting,* San Jose, California, November 1991, paper TuB4, post-deadline paper.

particularly efficient in certain semimetals and semiconductors (e.g., Bi, Sb, Te and Ti_2O_3).[14]

For our experiments we used pulses from a dispersion-balanced colliding-pulse-modelocked (CPM) dye laser, focused to a 2 μm spot. Reflectivity oscillations were observed in these materials with amplitudes of several percent. That is several orders of magnitude larger than can be expected from impulsive stimulated Raman scattering. In each material only one oscillation frequency was observed, the one corresponding to the A_{1g} mode; and the phase of the amplitude was cosinusoidal with respect to excitation at $t=0$. All of these facts are inconsistent with a stimulated Raman mechanism. To explain them, we have proposed a new theory, dubbed displacive excitation of coherent phonons (DECP).[15] It attributes behavior to a rapid displacement of the ion equilibrium coordinates by the electronic excitation.

The temperature dependence of this effect in Ti_2O_3 is particularly interesting. In the range 300 K-570 K dramatic changes take place in Ti_2O_3 with respect to both its lattice and electronic properties, turning it from a semiconductor to a metal. In our femtosecond experiments, we have observed temperature dependent changes in the optical phonon frequency and electronic relaxation rate that are consistent with this transition. On a dynamic basis this may mean that the bandgap and conductivity of the material are being modulated at the 6 THz phonon frequency. Work in progress will test this hypothesis. Higher excitation levels may also make it possible to observe anharmonic lattice dynamics. In recent preliminary experiments with an amplified CPM system we have measured refractive index modulations at the phonon frequency of as much as 15 percent.

1.10 Femtosecond Studies of Superconductivity

Sponsors

Joint Services Electronics Program
Contract DAAL03-89-C-0001
Contract DAAL03-92-C-0001
U.S. Air Force - Office of Scientific Research
Contract F49620-91-C-0091

Project Staff

Professor Erich P. Ippen, Tak K. Cheng, Siegfried B. Fleischer

Femtosecond optical experiments that monitor the rate of hot electron cooling in materials provide an estimate of the strength of the electron-phonon interaction. If one is dealing with BCS-like superconductors, and one knows the electron-phonon spectral density, femtosecond data on the cooling rate can be related directly to T_c. We have been successful in making such determinations in a range of metallic superconductors and in some high-T_c materials.[16] Recently, we have performed the first femtosecond pump-probe experiments on C_{60} and two of its intercalants.

Most of the properties of C_{60} and its intercalants can be explained by treating them as rolled up sheets of graphite. For this reason it is surprising that K_3C_{60} has a superconducting transition temperature (18 K) more than an order of magnitude higher than that of the other graphite intercalation compounds. Determining the reason for this difference may help develop a better understanding of the mechanisms leading to high-T_c.

For our experiments, thin films (1000Å) of C_{60}, K_3C_{60}, and K_6C_{60} were deposited on quartz substrates and encapsulated to prevent contamination. Femtosecond dynamics were induced and observed, in reflectivity and transmission at $\lambda = 630$ nm, using pulses from a colliding-pulse-modelocked (CPM) dye laser. We believe we are monitoring carrier cooling rates and have deduced time constants of 9 ps, 0.2 ps and 0.7 ps for the

[14] T.K. Cheng, J. Vidal, H.J. Zeiger, G. Dresselhaus, M.S. Dresselhaus, and E.P. Ippen, "Mechanism for Displacive Excitation of Coherent Phonons in Sb, Bi, Te, and Ti_2O_3," *Appl. Phys. Lett.* 59: 1923 (1991).

[15] H.J. Zeiger, J. Vidal, T.K. Cheng, E.P. Ippen, G. Dresselhaus, and M.S. Dresselhaus, "Theory for Displacive Excitation of Coherent Phonons," *Phys. Rev. B* 45: 768 (1992).

[16] S.D. Brorson, A. Kazeroonian, J.S. Moodera, D.W. Face, T.K. Cheng, E.P. Ippen, M.S. Dresselhaus, and G. Dresselhaus, "Femtosecond Room-temperature Measurement of the Electron-phonon Coupling Constant λ in Metallic Superconductors," *Phys. Rev. Lett.* 64: 2172 (1990); S.D. Brorson, A. Kazeroonian, D.W. Face, G.L. Doll, T.K. Cheng, M.S. Dresselhaus, G. Dresselhaus, E.P. Ippen, T. Venkatesan, X.D. Wu, and A. Inam. "Femtosecond Thermomodulation Study of high-T_c," *Solid. State Commun.* 74: 1305 (1990).

three samples, respectively. As might be expected, the superconducting sample has the shortest time constant. But the absolute value of the rate, in the context of the material's phonon spectral density, is surprisingly low for a T_c of 18 K. One possible explanation is that electron-phonon coupling is specific to certain types of phonons. This will be investigated by experiments with different material compositions as well as by more detailed studies of these particular intercalants.

1.11 Femtosecond Pulse Generation in Solid State Lasers

Sponsors

Joint Services Electronics Program
Contract DAAL03-89-C-0001
Contract DAAL03-92-C-0001
National Science Foundation
Grant ECS 85-52701
U.S. Air Force - Office of Scientific Research
Contract F49620-88-C-0089
U.S. Navy - Office of Naval Research
Contract N00014-91-C-0084

Project Staff

Dr. Guiseppe Gabetta, Joseph M. Jacobson, David Huang, Malini Ramaswamy, Professor Hermann A. Haus, Professor Erich P. Ippen, Professor James G. Fujimoto

1.11.1 Introduction

Ultrashort pulse laser technology is of primary importance for the development of high speed optical communication and measurement techniques and for studies of ultrafast phenomena. The principle objectives of our research program are the investigation and development of new ultrashort laser pulse generation and measurement techniques. Special emphasis is placed on studies of solid state ultrashort pulse laser technology. Solid state lasers represent a third generation technology that has several advantages over existing dye-laser technology. Solid state lasers feature lower cost, greater compactness, higher power, and broader tunability. The large gain bandwidths of solid state laser media can support pulse durations in the femtosecond range with wavelength tunability. These features make solid state laser technology a versatile tool for engineering and research applications in ultrafast phenomena.

One of the most promising solid state laser materials that has emerged to date is $Ti:Al_2O_3$.[17] The $Ti:Al_2O_3$ laser operates at room temperature, has a high energy storage suitable for high power operation, and a broad gain bandwidth with an extremely wide tuning range from 670 to 1000 nm. These features make it an ideal system for femtosecond pulse generation and spectroscopy.

Recently, we have developed and demonstrated a new ultrashort pulse generation technique known as Additive Pulse Modelocking (APM).[18] Self starting, passive modelocking was demonstrated in $Ti:Al_2O_3$ and pulse durations of 200 fs were achieved.[19] An APM laser utilizes an external cavity containing a nonlinear element such as an optical fiber to produce a pulse shortening mechanism similar to saturable absorber action. A saturable absorber is a nonlinear element that exhibits greater transmittivity or reflectivity for higher intensities. This nonlinearity produces pulse shortening by enhancing the peak of the pulse compared to the wings.

Our research in modelocked $Ti:Al_2O_3$ represented the first demonstration of self starting passive Additive Pulse Modelocking. The self-starting APM system represented a significant advancement because it eliminated the need for a high frequency loss modulation element and thus reduced system complexity and cost. We have extended the self-starting APM technique to modelock diode pumped laser systems and have generated 1.7 ps pulses in a Nd:YAG system and 2 ps pulses in a Nd:YLF system.[20]

---

[17] P.F. Moulton, "Spectroscopic and Laser Characteristics of $Ti:Al_2O_3$," *J. Opt. Soc. Am. B* 3: 125 (1986).

[18] E.P. Ippen, "Additive Pulse Modelocking," *J. Opt. Soc. Am. B* 6: 1736-1745 (1989); J. Goodberlet, J. Wang, J.G. Fujimoto, and P.A. Schulz, "Femtosecond Passive Modelocked $Ti:Al_2O_3$ Laser with a Nonlinear External Cavity," *Opt. Lett.* 14: 1125 (1989).

[19] J. Goodberlet, J. Wang, J.G. Fujimoto, and P.A. Schulz, "Femtosecond Passive Modelocked $Ti:Al_2O_3$ Laser with a Nonlinear External Cavity," *Opt. Lett.* 14: 1125 (1989).

[20] J. Goodberlet, J. Jacobson, J.G. Fujimoto, P.A. Schulz, and T.Y. Fan, "Self-starting Additive-pulse Mode-locked Diode-pumped Nd:YAG Laser," *Opt. Lett.* 15: 504-506 (1990).

1.11.2 Femtosecond Generation Using Nonlinear Intracavity Elements

Studies by other investigators have recently demonstrated that a single cavity $Ti:Al_2O_3$ system can be modelocked without an active modulator, saturable absorber, or nonlinear external cavity.[21] This phenomena was termed self-modelocking. Although these investigations did not elucidate the short pulse generation mechanisms, they demonstrated that a solid state laser could be modelocked solely by intracavity optical nonlinearities.

Solid state femtosecond lasers such as $Ti:Al_2O_3$ can achieve peak intracavity intensities of 0.5 MW when they are modelocked. These high peak intensities make possible a wide range of new modelocking techniques which utilize intracavity nonlinearities. Saturable absorber action based on all-optical solid state refractive index nonlinearities is of particular interest because of its extremely fast response and recovery times. Our group has pursued this approach further and demonstrated two different types of passive modelocking schemes in $Ti:Al_2O_3$ using all solid state nonlinear intracavity modulators.[22] These modelocking techniques permit the generation of femtosecond pulse durations and can be extended to a wide range of solid state lasers at different wavelengths. In addition, they represent a significant reduction in cost and system complexity over previous modelocking techniques.

One approach for modelocking uses a nonlinear intracavity element which functions by nonlinear polarization rotation. This device is called a Kerr Polarization Modulator (KPM)[23] and consists of a quarter-wave plate, a focusing lens, an SF11 glass plate, a second quarter-wave plate, and a curved end mirror. The KPM works by generating an elliptical polarization state which undergoes a nonlinear rotation due to the intensity dependent refractive index of the SF11 glass plate. The linear and nonlinear transmission functions of the KPM can be controlled by setting the retardations of the quarter-wave plates. Thus the KPM can be made to have an increasing transmission with increasing intensity and function as a saturable absorber. We have demonstrated this technique for modelocking $Ti:Al_2O_3$ and achieved pulse durations of 230 fs.

Another approach for modelocking relies on the use of intracavity self focusing. This technique has been termed Kerr Lens Modelocking (KLM),[24] and pulse durations in the 100 fs range have been demonstrated in $Ti:Al_2O_3$. KLM produces a fast saturable-like action by using self focusing in the laser rod combined with intracavity aperaturing. Research in our group has emphasized developing both a fundamental understanding of the underlying nonlinear processes as well as an approach for engineering these systems. We have introduced a significant simplification in the design of KLM lasers by developing a modular nonlinear intracavity element called a micro-dot mirror.[25]

The end mirror of the laser is substituted with a focusing lens and a mirror with small diameter micro-dots. The mirror is antireflection (AR) coated on the first surface (i.e., the surface that laser beam first encounters) and high reflection (HR) coated on the second surface. The second surface is patterned into an array of HR spots (micro-dots) with varying diameter using microelectronic techniques. Fast saturable absorber action is produced by nonlinear self focusing which produces a smaller spot size for higher intensities. When a pulse is reflected from the micro-dot mirror, the higher intensity peaks of the pulse are reflected more than the lower intensity

---

21 D.E. Spence, P.N. Kean, and W. Sibbett, "60-fsec Pulse Generation from a Self-mode-locked Ti:sapphire Laser," *Opt. Lett.* 16: 42 (1991).

22 G. Gabetta, D. Huang, J. Jacobson, M. Ramaswamy, H.A. Haus, E.P. Ippen, and J.G. Fujimoto, "Femtosecond Pulse Generation in $Ti:Al_2O_3$ Using Nonlinear Intracavity Elements," CLEO 1991, Baltimore, Maryland, 1991; G. Gabetta, D. Huang, J. Jacobson, M. Ramaswamy, H.A. Haus, E.P. Ippen, and J.G. Fujimoto, "Femtosecond Pulse Generation in $Ti:Al_2O_3$ Using a Microdot Mirror Modelocker," *Opt. Lett.* 16: 1756 (1991).

23 G. Gabetta, D. Huang, J. Jacobson, M. Ramaswamy, H.A. Haus, E.P. Ippen, and J.G. Fujimoto, "Femtosecond Pulse Generation in $Ti:Al_2O_3$ Using Nonlinear Intracavity Elements," CLEO 1991, Baltimore, Maryland, 1991.

24 D.K. Negus, L. Spinelli, N. Goldblatt, and G. Feugnet, "Sub-100 Femtosecond Pulse Generation by Kerr Lens Modelocking in $Ti:Al_2O_3$," OSA Meeting on Advanced Solid State Lasers, Hilton Head, South Carolina, March 18-20, 1991, postdeadline paper.

25 G. Gabetta, D. Huang, J. Jacobson, M. Ramaswamy, H.A. Haus, E.P. Ippen, and J.G. Fujimoto, "Femtosecond Pulse Generation in $Ti:Al_2O_3$ Using a Microdot Mirror Modelocker," *Opt. Lett.* 16: 1756 (1991); D. Huang, M. Ulman, L. Acioli, H.A. Haus, and J.G. Fujimoto, "Self-focusing Induced Saturable Absorber Loss for Laser Mode Locking," *Opt. Lett.*, forthcoming.

wings of the pulse. Thus the micro-dot mirror effectively acts as a fast saturable absorber. We have demonstrated the micro-dot mirror for modelocking the Ti:Al_2O_3 laser and achieved pulse durations of 190 fs.

The modelocking techniques described above have led to a better understanding of passive modelocking mechanisms in solid state laser systems. In the case of self-focusing modelocking, we developed a new theoretical framework which is applicable to the majority of single cavity passively modelocked Ti:Al_2O_3 systems.[26] Theoretical studies are important not only for understanding pulse shortening mechanisms but also for investigating factors which limit pulse duration.

We have developed an analytical description of modelocking which includes fast saturable absorption, self phase modulation, gain bandwidth limiting, and dispersion. A pulse in a modelocked laser can be mathematically described by a single equation similar to the nonlinear Schrodinger equation. We have studied the behavior of pulse characteristics such as pulse duration, chirp, bandwidth, and stability.[26] Our primary findings show that there are two basic operating regimes where stable short pulse generation may be achieved. A laser may be constructed either with positive (normal) or negative (anomalous) dispersion. The pulse shaping mechanisms for these two regimes are different and a laser that has anomalous dispersion will in general produce dramatically shorter pulses than one with normal dispersion. These results suggest design criteria for a wide range of modelocked solid state lasers.

1.11.3 Reduction of Pulse Duration by Dispersion Compensation

One of the key topics of investigation in ultrashort pulse generation is the development of approaches for generating the shortest possible pulse durations. The fundamental limit to pulse duration is determined by the energy-time uncertainty principle which implies that the pulse duration is inversely related to the laser gain bandwidth. The gain bandwidth in Ti:Al_2O_3 is in excess of 100-200 nm[27] and thus pulse durations of a few femtoseconds are theoretically possible. Pulse compression techniques using amplified femtosecond pulses have been demonstrated to achieve pulses as short as 6 fs.[28] However, pulses in the 10 fs range have not as yet been generated directly from a laser. The broad bandwidths associated with these pulse durations allow the use of frequency synthesis techniques to control pulse shape or generate multiple pulse, multiple wavelength pulse trains.[29] Thus, the development of new sources with pulse durations in the 10 fs range would have a major impact on the study of ultrafast phenomena.

One area of investigation in our program is the exploration of the factors which limit the short pulse duration that can be generated. The theoretical considerations discussed above are valid only in systems where the pulses are long enough that dispersive terms higher than those of second order can be neglected. Previous pulse compression studies have demonstrated that higher order dispersion presents an important limitation to pulse duration as pulses become very short and their corresponding frequency bandwidths become broad.[30]

In order to explore and extend the limits of short pulse generation, we have developed and demonstrated a solid state laser with independently adjustable second and third order dispersion. Compensation of dispersion is achieved using a pair of intracavity prisms which are set to produce a net negative second order dispersion in the

[26] H.A. Haus, J.G. Fujimoto, and E.P. Ippen, "Structures for Additive Pulse Modelocking," *J. Opt. Soc. Am. B* 8: 2068 (1991).

[27] P.F. Moulton, "Spectroscopic and Laser Characteristics of Ti:Al_2O_3," *J. Opt. Soc. Am. B* 3: 125 (1986).

[28] R.L. Fork, C.H. Brito Cruz, P.C. Becker, and C.V. Shank, "Compression of Optical Pulses to Six Femtoseconds by Using Cubic Phase Compensation," *Opt. Lett.* 12: 483 (1987).

[29] A.M. Weiner, J.P. Heritage, and E.M. Kirschner, "High-resolution Femtosecond Pulse Shaping," *J. Opt. Soc. Am. B* 5: 1563 (1988).

[30] W.J. Tomlinson and W.H. Knox, "Limits of Fiber-grating Optical Pulse Compression," *J. Opt. Soc. Am. B* 4: 1404 (1987); C.H. Brito Cruz, P.C. Becker, R.L. Fork, and C.V. Shank, "Phase Correction of Femtosecond Optical Pulses Using a Combination of Prisms and Gratings," *Opt. Lett.* 13: 123 (1988).

cavity. Intracavity prisms are a standard technique for dispersion compensation which have been applied to a number of solid state and dye lasers. An undesirable consequence of this prism arrangement, however, is that it also introduces a significant negative third order dispersive term which produces pulse distortion effects.[30] In order to explicitly compensate for third order dispersion, we have developed an intracavity thin film element which has positive third order dispersion but zero second order dispersion. Working in collaboration with investigators at CVI Incorporated, we designed and fabricated a thin film Gires-Tourneau Interferometer (GTI) on a mirror substrate. The amount of third order compensation introduced in the laser cavity can be varied by adjustment of the number of times the pulse bounces off each GTI surface during each round trip. This is the first laser that has directly adjustable second and third order dispersion. Using this technique we have generated pulse durations as short as 28 fs directly from a modelocked $Ti:Al_2O_3$ laser. These pulses are the shortest pulses which have been directly generated from a $Ti:Al_2O_3$ laser without using pulse compression techniques.[31]

1.12 Studies of Ultrafast Phenomena in Optoelectronic Materials

Sponsors

Joint Services Electronics Program
  Contract DAAL03-89-C-0001
  Contract DAAL03-92-C-0001
National Science Foundation
  Grant ECS 85-52701
U.S. Air Force - Office of Scientific Research
  Contract F49620-88-C-0089
U.S. Navy - Office of Naval Research
  Grant N00014-91-J-1956

Project Staff

Dr. Lucio H. Acioli, Morrison Ulman, David Huang, Professor Erich P. Ippen, Professor James G. Fujimoto

1.12.1 Four Wave Mixing and Temporal Encoding in Barium Titanate

The idea of optically encoding information in photosensitive materials is relevant to applications in optical signal processing, image processing, and optical logic. Holography is an example of a technique in which three-dimensional spatial information can be recorded in a suitable matrix such as film or photorefractive material. In addition to spatial information, temporal information may also be encoded. The search for systems to record information in the temporal domain have usually been based on the concept of encoding information using inhomogeneously broadening transitions in atomic systems. The techniques most often applied for temporal storage have been variations of photon echo like schemes. Working in collaboration with investigators from Tufts University, we have performed the first studies of femtosecond wave-mixing in $BaTiO_3$ and demonstrated the possibility of using volume holography for recording temporal information.[32]

Photorefractive materials such as $BaTiO_3$, or SBN, have been demonstrated for a wide range of optical phase conjugation and signal processing experiments using continuous wave lasers.[33] These materials exhibit extremely large nonlinearities, and studies can be performed without the need for high laser intensities. However, the response and relaxation times of the photorefractive materials are extremely slow, and thus only recently has the use of such materials under pulsed laser excitation been considered. In order to circumvent the slow material response, our technique records temporal information in the spatial domain using four wave mixing and modulated volume photorefractive gratings.

Experiments were performed using a colliding pulse modelocked, CPM, dye laser source which generated 40 fs pulse durations. Temporal information was encoded using a signal and a reference beam. When the signal and reference beams interact in the photorefractive crystal, they form a

---

31 J.M. Jacobson, A.G. Jacobson, K. Naganuma, and J.G. Fujimoto, "Generation of 28 fs Pulses from a $TiAl_2O_3$ Laser Using Second and Third Order Intracavity Dispersion Compensation," paper to be presented at CLEO 1992, Anaheim, California.

32 L.H. Acioli, M. Ulman, E.P. Ippen, J.G. Fujimoto, H. Kong, B.S. Chen, and M. Cronin-Golomb, "Femtosecond Temporal Encoding in Barium Titanate," *Opt. Lett.* 16: 1984 (1991).

33 M. Cronin-Golomb, B. Fischer, J.O. White, and A. Yariv, "Theory and Applications of Four-wave Mixing in Photorefractive Media," *IEEE J. Quant. Electron.* QE-20: 12 (1984).

standing wave interference pattern where they geometrically overlap. This in turn induces a photorefractive diffraction grating. If the signal beam contains a femtosecond temporal waveform, and the reference beam consists of a single femtosecond pulse, a spatially varying interference pattern will be formed according to the geometrical overlap of the signal and the reference optical waveforms. The temporal information on the signal beam is recorded as a volume grating in the $BaTiO_3$ crystal. The photorefractive gratings have a long persistence time and can be used to store the temporal information. The femtosecond waveform can subsequently be reconstructed by diffracting a femtosecond reference pulse from the stored volume grating.[34] This process is analogous to image reconstruction in holography.

Different phase conjugation geometries were examined including the ring resonator and the two beam coupling geometry. A surprising discovery was that temporal signals are influenced only by material dispersion effects and that pulse durations of 40 fs could be preserved. We have determined that the factors that influence the temporal resolution of the temporal encoding and reconstruction process and developed a simple geometrical model to predict resolution and information storage capacity. Our experiments are closely related to femtosecond holography which uses holographic recording to store transient femtosecond images,[35] except that our results demonstrate an extension of this technique to both the storage and reconstruction of temporal information. Variations of our approach using acousto-optic modulators or other programmable volume diffraction devices could make possible the generation of programmable optical pulses at THz repetition rates.

1.12.2 Self-Focusing and Nonlinear Propagation

Nonlinear optical media with Kerr-like refractive index nonlinearities are relevant to a wide range of applications including all-optical switching, optical modulation, short pulse generation, and short pulse propagation in optical fibers. Self-focusing is a classic nonlinear optical process which has been the subject of investigation for many years. This process has been of interest in previous studies because it poses a limitation to high power laser generation. Recently, however, self-focusing has become technologically important for applications which involve high speed all-optical modulation and short pulse generation. A new technique for modelocking solid state lasers, called Kerr lens modelocking has been developed which uses self focusing to achieve fast saturable absorber action.[36] Pulse durations of less than 100 fs have been achieved in the $Ti:Al_2O_3$ laser. Self-focusing also plays a major role in other short pulse generation techniques such as high power femtosecond pulse compression and continuum generation.[37]

Self-focusing is produced by the intensity dependent nonlinear index of refraction of the material and the spatial intensity variation of the laser beam. The transverse spatial intensity variation of the beam induces a graded index lens in the nonlinear material which, in turn, produces a geometric focusing of the beam. Several researchers have studied this problem in the past, and, with the advent of high intensity femtosecond lasers, a description of the temporal as well as the spatial behavior of self-focusing has become of interest. There is no theory yet that fully describes the problem of nonlinear femtosecond pulse propagation in bulk nonlinear media.

Our investigations of self-focusing are directed toward applications in laser modelocking and short pulse generation. Self-focusing has recently been used to achieve fast saturable absorber mode-

---

[34] L.H. Acioli, M. Ulman, E.P. Ippen, J.G. Fujimoto, H. Kong, B.S. Chen, and M. Cronin-Golomb, "Femtosecond Temporal Encoding in Barium Titanate," *Opt. Lett.* 16: 1984 (1991).

[35] J.A. Valdmanis, H. Chen, E.N. Leith, Y. Chen, and J.L. Lopez, "Three Dimensional Imaging with Femtosecond Optical Pulses," *CLEO Technical Digest* paper CTUA1, 1990, p. 54.

[36] D.K. Negus, L. Spinelli, N. Goldblatt, and G. Feugnet, "Sub-100 Femtosecond Pulse Generation by Kerr Lens Modelocking in $Ti:Al_2O_3$," OSA Meeting on Advanced Solid State Lasers, Hilton Head, South Carolina, March 18-20, 1991, postdeadline paper.

[37] C. Rolland and P.B. Corkum, "Compression of High-power Optical Pulses," *J. Opt. Soc. Am. B* 5: 641 (1988); D.H. Reitze, A.M. Weiner, and D.E. Leaird, "High-power Femtosecond Optical Pulse Compression by Using Spatial Solitons," *Opt. Lett.* 16: 1409 (1991); R.L. Fork, C.V. Shank, C. Hirlimann, R. Yen, and W.J. Tomlinson, "Femtosecond White-light Continuum Pulses," *Opt. Lett.* 8: 1 (1983).

locking in $Ti:Al_2O_3$. This process has been termed Kerr Lens Modelocking and can form the basis for ultrashort pulse generation in a wide range of solid state lasers.[38] As discussed previously, we have developed a modular device called a micro-dot mirror which uses self-focusing to modelock the $Ti:Al_2O_3$ laser.[39] In addition, self-focusing in bulk materials can also be used for short pulse generation and nonlinear measurement. High power pulse compression has been demonstrated using self phase modulation in bulk nonlinear materials.[40] It has also been shown that self-focusing plays a fundamental role in the process of continuum generation with femtosecond pulses and can be used to generate spatial optical solitons for pulse compression.[41] An experimental technique, based on the self-focusing effect and referred to as "z-scan,"[42] has been introduced as a sensitive probe of the magnitude of the nonlinear refractive index.

In order to investigate the use of self-focusing for modelocking and ultrashort pulse propagation, we have developed a new approach to describe the effects of self-focusing in thick (compared to the confocal parameter of the beam) nonlinear media.[43] This method is based on a complex scaling operation applied to the q parameter of a gaussian beam. Self-focusing can be described in the perturbative limit using a compact formulation that is compatible with the ABCD matrix description of gaussian beam propagation. Experimental "z-scan" measurements of self-focusing were performed using a femtosecond CPM (colliding pulse modelocked) dye laser and high repetition rate copper vapor laser pumped amplifier.[44] Excellent agreement between the theoretical predictions and the experimental results have been obtained for thick optical glasses (BK7 and fused silica). These theoretical and experimental studies provide a basis for designing and developing Kerr lens modelocking techniques in a wide range of solid state lasers.

We have also studied the effects of self-focusing in continuum generation. Our investigations use variations of the "z-scan" technique[45] in order to quantify the continuum generation process by varying the nonlinear propagation parameters of the beam. Our current studies focus on describing energy transfer to wavelengths different from that of the input beam, the amplitude stability, and the divergence properties of the output beam. An increased understanding of these processes can form the basis for developing new short pulse generation techniques based on nonlinear propagation.

1.12.3 Femtosecond Carrier Dynamics in Semiconductors

The efficient design of high speed electronic and photonic devices requires a detailed understanding of transient carrier dynamics in semiconductor materials. The dynamics of electrons and holes determine fundamental limitations to device speed. For example, intervalley scattering processes affect

---

[38] D.K. Negus, L. Spinelli, N. Goldblatt, and G. Feugnet, "Sub-100 Femtosecond Pulse Generation by Kerr Lens Modelocking in $Ti:Al_2O_3$," OSA Meeting on Advanced Solid State Lasers, Hilton Head, South Carolina, March 18-20, 1991, postdeadline paper.

[39] G. Gabetta, D. Huang, J.M. Jacobson, M. Ramaswamy, E.P. Ippen, and J.G. Fujimoto, "Femtosecond Pulse Generation in $Ti:Al_2O_3$ Using a Microdot Mirror Mode Locker," *Opt. Lett.* 16: 1756 (1991).

[40] C. Rolland and P.B. Corkum, "Compression of High-power Optical Pulses," *J. Opt. Soc. Am. B* 5: 641 (1988); D.H. Reitze, A.M. Weiner, and D.E. Leaird, "High-power Femtosecond Optical Pulse Compression by Using Spatial Solitons," *Opt. Lett.* 16: 1409 (1991).

[41] D.H. Reitze, A.M. Weiner, and D.E. Leaird, "High-power Femtosecond Optical Pulse Compression by Using Spatial Solitons," *Opt. Lett.* 16: 1409 (1991); R.L. Fork, C.V. Shank, C. Hirlimann, R. Yen, and W.J. Tomlinson, "Femtosecond White-light Continuum Pulses," *Opt. Lett.* 8: 1 (1983).

[42] M. Sheik-Bahae, A.A. Said, T. Wei, D.J. Hagan, and E.W. Van Stryland, "Sensitive Measurement of Optical Nonlinearities Using a Single Beam," *IEEE J. Quant. Electron.* 26: 760 (1990).

[43] D. Huang, M. Ulman, L. Acioli, H.A. Haus, and J.G. Fujimoto, "Self-focusing Induced Saturable Absorber Loss for Laser Mode Locking," *Opt. Lett.*, forthcoming.

[44] R.L. Fork, C.V. Shank, C. Hirlimann, R. Yen, and W.J. Tomlinson, "Femtosecond White-light Continuum Pulses," *Opt. Lett.* 8: 1 (1983).

[45] M. Sheik-Bahae, A.A. Said, T. Wei, D.J. Hagan, and E.W. Van Stryland, "Sensitive Measurement of Optical Nonlinearities Using a Single Beam," *IEEE J. Quant. Electron.* 26: 760 (1990).

the high field transport behavior of GaAs devices.[46] Carrier dynamics have been studied with a number of techniques including luminescence spectroscopy and femtosecond absorption saturation.[47] Our research program combines state-of-the-art experimental and theoretical approaches to develop an accurate model for carrier dynamics on an ultrashort timescale. The ultrahigh temporal resolution of femtosecond lasers permits direct measurement of electronic scattering processes that occur in less than 100 femtoseconds. Carrier scattering events may be examined both experimentally and by supercomputer simulation. As a result of these investigations, transient electronic behavior in a variety of important semiconductor materials and quantum structures may be predicted. Recently, we have focused our efforts on intervalley scattering in AlGaAs as a paradigm for investigating femtosecond carrier dynamics.

Our research program is a collaborative effort with Professor C.J. Stanton's solid state theory group at the University of Florida. The objective of the theoretical component of the program is to develop both numerical simulation and analytical methods which establish a correspondence between experimental femtosecond transient absorption saturation results and theoretical models. The problem of investigating transient carrier dynamics in III-V semiconductors is extremely complicated because of the large number of scattering processes. Thus, advanced theoretical techniques such as Ensemble Monte Carlo theory are necessary to accurately interpret experimental results. A full zone, 30 band, empirical $k \bullet p$ procedure is used to determine the relevant electronic bandstructure. A Monte Carlo simulation of 40,000 electrons and holes tracks the time development of the electron and hole distribution functions. Finally, the differential transmission is calculated and compared directly to the results of femtosecond pump-probe experiments.[48] In this way, fundamental material parameters such as deformation potential constants and carrier-carrier scattering rates may be determined. An analytic discretization of the Boltzmann equation combined with a rate equation approach has also been developed to provide intuitive insight into the transient carrier relaxation process. This interdisciplinary approach has already shown that collisional broadening and femtosecond hole redistribution must be included in the theory in order to match the experimental results. We are now investigating the role of carrier diffusion and coulomb enhancement on the differential transmission data.

In the past year, work at MIT has been directed toward femtosecond pump-probe absorption saturation studies of the GaAs and AlGaAs semiconductor systems. Femtosecond intervalley scattering in AlGaAs is investigated using a tunable wavelength technique. Systematic variation of the wavelength and spectral content of ultrashort laser pulses permits a selective study of different scattering channels, such as scattering to the L satellite valley. An amplified colliding pulse modelocked (CPM) ring dye laser system provides the source for our experiments. Femtosecond optical pulses from the CPM are amplified by a copper vapor laser pumped dye amplifier to microjoule energies. The amplified pulses are focused on a jet of ethylene glycol to generate a femtosecond white light continuum using nonlinear self phase modulation. A Fourier synthesis scheme selects variable wavelengths and pulse durations for use in pump-probe experiments.[49] This approach has the advantage that it permits studies using wavelength tunable pulses with durations as short as 30 fs. The samples used in our studies are grown by molecular beam epitaxy at MIT Lincoln Laboratory. The mole fraction of Al in the $Al_xGa_{1-x}As$ system is chosen to vary the bandstructure and isolate optical transitions of interest. Scattering to the L valley in $Al_{0.1}Ga_{0.9}As$ is only allowed for photoexcited carriers with energy greater than 1.8 eV. The possibility of scattering by this channel affects the behavior of the transient in femtosecond absorption saturation.

---

[46] M.A. Littlejohn, J.R. Hauser, T.H. Glisson, D.K. Ferry, and J.W. Harrison, "Alloy Scattering and High Field Transport in Ternary and Quaternary III-V Semiconductors," *Solid State Electron.* 21: 107 (1978).

[47] S.A. Lyon, "Spectroscopy of Hot Carrier in Semiconductors," *J. Lumines.* 35: 121-154 (1986); J. Shah, B. Deveaud, T.C. Damen, and W.T. Tsang, "Determination of Intervalley Scattering Rates in GaAs by Subpicosecond Luminescence Spectroscopy," *Phys. Rev. Lett.* 59: 2222-2225 (1987); R.G. Ulbrich, J.A. Kash, and J.C. Tsang, "Hot-electron Recombination at Neutral Acceptors in GaAs: A cw Probe of Femtosecond Intervalley Scattering," *Phys. Rev. Lett.* 62: 949-952 (1989); P.C. Becker, H.L. Fragnito, C.H. Brito Cruz, R.L. Fork, J.E. Cunningham, J.E. Henry, and C.V. Shank, "Femtosecond Intervalley Scattering in GaAs," *Appl. Phys. Lett.* 53: 2089-2090 (1988).

[48] C.J. Stanton and D.W. Bailey, "Evaluating Photoexitation Experiments Using Monte Carlo Simulations," in *Monte Carlo Simulations of Semiconductors and Semiconductor Devices,* ed. K. Hess (Boston: Klunker Academic, 1991).

[49] A.M. Weiner, J.P. Heritage, and E.M. Kirschner, "High Resolution Femtosecond Pulse Synthesis," *J. Opt. Soc. Am. B* 5: 1563 (1988).

Thus, a wavelength tunable study discerns salient features of the data in both the time and energy dimensions.

The results already obtained will be extended to new materials systems and to quantum confined structures. Device design in the future will depend on thorough knowledge of the transient electronic properties of semiconductor materials. The combination of advanced femtosecond laser technology with sophisticated theoretical methods provides a potent tool for discovery of fundamental information on ultrafast carrier dynamics.

1.13 Time Domain Diagnostics of Waveguide Devices

Sponsors

Joint Services Electronics Program
Contract DAAL03-89-C-0001
Contract DAAL03-92-C-0001
National Science Foundation
Grant ECS 85-52701
U.S. Air Force - Office of Scientific Research
Contract F49620-88-C-0089

Project Staff

Claudio D.C. Chamon, Chi-Kuang Sun, Professor Hermann A. Haus, Professor James G. Fujimoto

1.13.1 Time Domain Interferometry

Investigations of nonlinear processes such as measurements of the nonlinear index of refraction in waveguide devices are key to the development of high speed all-optical switching devices. In particular, the magnitude of the nonlinear index is an important parameter for all-optical switching and modulation, since it determines the laser pulse energy which is necessary to achieve switching behavior. Time domain measurements permit both the magnitude as well as the dynamics of the nonlinear index of refraction to be characterized. Previous investigators have used a number of time or frequency domain techniques to measure nonlinear index including four wave mixing,[50] nonlinear waveguide couplers,[51] nonlinear Fabry-Perots,[52] fringe shift interferometry,[53] and Mach-Zehnder interferometry.[54] In general, direct measurements of index nonlinearities are complicated because measurement techniques are sensitive to thermal or acoustical parasitic signals, have low sensitivity, or require deconvolution.

Recently, we have developed a new technique, femtosecond time division interferometry (TDI), that permits high sensitivity, direct measurements of the nonlinear index n_2 in waveguide devices with reduced interference from thermal or acoustical parasitic signals.[55] In this technique, pump and probe pulses are coupled into a waveguide device and the nonlinear phase shift which is induced on the probe by the pump is measured by interfering it with a reference pulse. TDI was previously limited to measurements of $n_{2\perp}$, i.e., index changes induced on a probe pulse by an orthogonally polarized pump. However, new materials such as quantum wells, quantum wires, organic polymers as well as other anisotropic systems are

---

[50] W.K. Burns and N. Bloembergen, "Third-harmonic Generation in Absorbing Media of Cubic or Isotropic Symmetry," *Phys. Rev. B* 4: 3437 (1971).

[51] P. Li, K. Wa, J.E. Sitch, N.J. Mason, J.S. Roberts, and P.N. Robson, "All Optical Multiple-quantum-well Waveguide Switch," *Electron. Lett.* 21: 27 (1985).

[52] Y.H. Lee, A. Chavez-Pirson, S.W. Koch, H.M. Gibbs, S.H. Park, J. Morhange, A. Jeffrey, N. Peyghambarian, L. Banyai, A.C. Gossard, and W. Wiegmann, "Room Temperature Optical Nonlinearities in GaAs," *Phys. Rev. Lett.* 57: 2446 (1986).

[53] G.R. Olbright and N. Peyghambarian, "Interferometric Measurement of the Nonlinear Index of Refraction, n_2, of CdS_xSe_{1-x}-doped Glasses," *Appl. Phys. Lett.* 48: 1184 (1986).

[54] D. Cotter, C.N. Ironside, B.J. Ailslie, and H.P. Girdlestone, "Picosecond Pump Probe Interferometric Measurement of Optical Nonlinearity in Semiconductor Doped Fibers," *Opt. Lett.* 14: 317 (1989).

[55] M.J. LaGasse, K.K. Anderson, H.A. Haus, and J.G. Fujimoto, "Femtosecond All-optical Switching in AlGaAs Waveguides Using a Single Arm Interferometer," *Appl. Phys. Lett.* 54: 2068 (1989); M.J. LaGasse, K.K. Anderson, C.A. Wang, H.A. Haus, and J.G. Fujimoto, "Femtosecond Measurements of the Nonresonant Nonlinear Index in AlGaAs," *Appl. Phys. Lett.* 56: 417 (1990).

becoming increasingly important candidates for all optical switching devices. A complete characterization of n_2 requires the measurement of $n_{2\parallel}$.

During the past year, we have developed a new variation of our original time division interferometry, TDI, technique which permits the complete characterization of the nonlinear index.[56] By using a novel phase modulation technique which breaks the degeneracy between the pump and probe and actively stabilizes the interferometer, the magnitude and femtosecond transient response of $n_{2\parallel}$ can be measured. Experiments have been performed to measure $n_{2\perp}$ and $n_{2\parallel}$ in an optical fiber to demonstrate this new measurement technique. High sensitivities have also been achieved and phase shifts as small as 5 milirad can easily be detected. Thus, TDI can be applied to studies of nonlinear index and all-optical switching in a wide range of waveguide devices.

1.13.2 Time Domain Diagnostics of Strained Layer Devices

Strained layer quantum well devices represent one of the most active and technologically promising areas of current optoelectronics device research. Strained layer materials greatly extend the available wavelength range of optoelectronic devices by permitting the growth of non-lattice materials. In addition, strained layer materials represent a bandgap engineering approach to achieve superior device performance. By modifying the valence band structure, lower threshold current density, higher efficiency, smaller chirp, wider modulation bandwidth, and improved high temperature performance[57] can be achieved over conventional devices.[58] High power, high efficiency, long lifetime, and low threshold current density[59] semiconductor lasers have been achieved in InGaAs strained layer devices. With their extended wavelength range and high output power, InGaAs/GaAs strained layer lasers are important for applications such as coherent optical communications, pumping erbium doped fiber amplifier and solid state lasers, and high speed optical signal processing.

With the development of new tunable femtosecond laser source of wavelengths between 900 and 1000 nm, time domain diagnostics can become a powerful tool for characterizing dispersion, gain dynamics, nonlinear index change, and transient nonlinearities. We have recently begun a program in collaboration with Groups 67 and 83 at Lincoln Laboratory to develop frequency and time domain diagnostics of strained layer diode lasers. The objective of our program is twofold: To develop and demonstrate new time and frequency domain diagnostics of diode lasers, and to examine fundamental processes and device design issues which limit high power single frequency performance in strained layer diodes.

Studies will involve InGaAs/GaAs graded-index separate-confinement heterostructure strained layer single quantum well laser diodes.[60] Femtosecond pump probe measurements of gain dynamics, nonlinear index, and dispersion are being performed. Continous wave measurements such as linewidth, spectral character, self heterodyne four wave mixing, and injection locking are being performed at Lincoln Laboratory. These two approaches represent complementary techniques which, taken together, can permit a more comprehensive characterization of device and materials properties. When completed, this study should establish new approaches for performing time domain diagnostics on a wide range of devices as well as provide

---

[56] C. de C. Chamon, C. K. Sun, H.A. Haus, and J.G. Fujimoto, "Femtosecond Time Division Interferometry Technique for Measuring the Tensor Components of $\chi^{(3)}$," *Appl. Phys. Lett.*, forthcoming.

[57] N.K. Dutta, J. Lopata, D.L. Sivco, and A.Y. Cho, "Temperature Dependence of Threshold of Strained Quantum Well Lasers," *Appl. Phys. Lett.* 58: 1125 (1991).

[58] E. Yablonovitch and E.O. Kane, "Reduction of Lasing Threshold Current Density by the Lowering of Valence Band Effective Mass," *J. Lightwave Technol.* LT-4: 504 (1986); A.R. Adams, "Band-structure Engineering for Low-threshold High-efficiency Semiconductor Lasers," *Electron. Lett.* 22: 249 (1986); I. Suemune, L.A. Coldren, M. Yamanishi, and Y. Kan, "Extremely Wide Modulation Bandwidth in a Low Threshold Current Strained Quantum Well Laser," *Appl. Phys. Lett.* 53: 1378 (1988).

[59] H.K. Choi and C.A. Wang, "InGaAs/AlGaAs Strained Single-quantum-well Diode Lasers with Extremely Low Threshold Current Density and High Efficiency," *Appl. Phys. Lett.* 57: 321 (1990); R.L. Williams, M. Dion, F. Chatenoud, and K. Dzurko, "Extremely Low Threshold Current Strained InGaAs/AlGaAs Lasers by Molecular Beam Epitaxy," *Appl. Phys. Lett.* 58: 1816 (1991).

[60] H.K. Choi and C.A. Wang, "InGaAs/AlGaAs Strained Single-quantum-well Diode Lasers with Extremely Low Threshold Current Density and High Efficiency," *Appl. Phys. Lett.* 57: 321 (1990).

information relevant to optimizing high power device performance in the InGaAs/GaAs system.

1.14 Laser Medicine and Surgery

Sponsors

Johnson and Johnson Research Grant
National Institutes of Health
 Contract 2-R01-GM35459
U.S. Navy - Office of Naval Research
 Contract N00014-91-C-0084

Project Staff

Dr. Joseph A. Izatt, Dr. Charles P. Lin, David Huang, Michael R. Hee, Professor James G. Fujimoto

1.14.1 The Ultrashort Pulse Laser Scalpel

In recent years, the use of short optical pulses has enhanced the degree of control and localizability of intraocular laser surgery.[61] Laser induced optical breakdown is a nonlinear laser tissue interaction which permits the photodisruption or cutting of transparent structures within the eye without the need for intervening surgical incision. The objective of our program is to develop an optimized ultrashort pulse laser scalpel which can be used to perform surgical incisions of intraocular structures even in close proximity to sensitive ocular structures such as the retina and cornea. These studies are part of an onging collaboration between investigators at MIT, the New England Eye Center of New England Medical Center Hospitals, and the Wellman Laboratories of Photomedicine at Massachusetts General Hospital.

The physical processes which occur in laser induced breakdown include plasma formation, acoustic wave generation, and cavitation. These processes produce the laser tissue surgical effects as well as collateral damage. To date, the majority of clinical applications of laser induced optical breakdown have utilized nanosecond duration pulses in the millijoule energy range and single pulse exposures. We have studied and compared the mechanisms, scaling behavior, and tissue effects of single pulses in the nanosecond and picosecond ranges.[62] In general, nanosecond and picosecond optical breakdown results in comparable damage zones if the same amount of energy is deposited; however, since the threshold energy for breakdown is much lower for picosecond pulses, near-threshold picosecond pulses produce greatly reduced collateral damage zones. For example, we have demonstrated collateral damage ranges in a corneal endothelial cell model of only 100 μm with 40 picosecond duration pulses at 8 microjoules pulse energy. We have also studied tissue effects (corneal excisions) into the femtosecond domain.[63] Ultrashort pulses with high peak intensities can produce a plasma mediated ablation of transparent tissues such as the cornea. Picosecond and femtosecond pulse durations have been demonstrated to produce much smoother excision edges and less damage to the adjacent tissue than nanosecond pulses.

We have demonstrated that clinically viable surgical incisions can be made using multiple pulse, high repetition rate picosecond pulses. Each pulse produces minimal collateral damage while multiple exposures produce a cumulative incision effect. In order to study the effect of repetition rate, we have developed a new Nd:YAG laser system which produces 100 picosecond duration pulses with a maximum energy of 140 μJ and a repetition rate variable from 3 to 1000 Hz. This laser has been used to demonstrate in vitro cutting of a monolayer of cultured fibroblast cells suspended over corneal endothelium in saline as a model for vitreous membrane surgery. Membrane cutting in the deep vitreous in close proximity to the retina remains one of the most challenging problems for

[61] F. Fankhauser, P. Roussel, J. Steffen, E. Van der Zypen, and A. Cherenkova, "Clinical Studies on the Efficiency of High Power Laser Radiation Upon Some Structures of the Anterior Segment of the Eye," *Int. Ophthalmol.* 3: 129 (1981).

[62] J.G. Fujimoto, W.Z. Lin, E.P. Ippen, C.A. Puliafito, and R.F. Steinert, "Time Resolved Studies of Nd:YAG Laser Induced Breakdown," *Invest. Ophthal. Vis. Sci.* 26: 1771 (1985); B. Zysset, J.G. Fujimoto, and T.F. Deutsch, "Time Resolved Measurements of Picosecond Optical Breakdown," *Appl. Phys. B* 48: 139 (1989); B. Zysset, J.G. Fujimoto, C.A. Puliafito, R. Birngruber, and T.F. Deutsch, "Picosecond Optical Breakdown: Tissue Effects and Reduction of Collateral Damage," *Lasers Surg. Med.* 9: 193 (1989); D. Stern, R. Schoenlein, C.A. Puliafito, E.T. Dobi, R. Birngruber, and J.G. Fujimoto, "Corneal Ablations by Nanosecond, Picosecond, and Femtosecond Lasers at 532 and 625 nm," *Arch. Ophthalmol.* 107: 587 (1989).

[63] D. Stern, R. Schoenlein, C.A. Puliafito, E.T. Dobi, R. Birngruber, and J.G. Fujimoto, "Corneal Ablations by Nanosecond, Picosecond, and Femtosecond Lasers at 532 and 625 nm," *Arch. Ophthalmol.* 107: 587 (1989).

vitreoretinal surgeons, despite advances in mechanical vitrectomy. In our experiments, efficient cutting of fibroblast cell membranes was observed by applying repetitive, 50-80 μJ pulses at 50-200 Hz while translating the membranes across the laser focus. Incision widths were as narrow as 5 cell diameters, or 50 μm, while membranes suspended as close as 200 μm over corneal endothelium could be incised without detectable damage to the endothelial cells. These experiments were followed up by in vivo incision of induced vitreous membranes in rabbit eyes. In these experiments, vitreous strands were cut at distances as close as 100 μm to the retina using 60-100 μJ pulses at 200 Hz. No retinal hemorrhages were observed, and histological examination of the underlying retina revealed only minor cell disruption. These results comprise considerable advances over the capabilities of nanosecond pulse duration photodisrupters in current clinical use.

1.14.2 Optical Coherence Domain Reflectometry in Biological Systems

Optical coherence domain reflectometry (OCDR) is a new noninvasive, noncontact ranging technique able to profile optical reflectivity versus depth in both transparent and scattering media.[64] OCDR employs a short coherence length light source and interferometric detection to determine the time-of-flight delay of light reflected from different points in a sample. The technique is the optical analog of ultrasound, but offers higher spatial resolution and noncontact measurement. OCDR uses heterodyne signal detection techniques common in high performance optical communication systems to achieve superior sensitivity and noise rejection. Unlike time-domain optical ranging techniques, OCDR only requires a small, low-power, superluminescent laser diode source and may be engineered into a safe, compact, clinically useful fiber optic device. We believe that OCDR has important clinical applications in laser microsurgery and medical diagnostics.

Working in collaboration with the Optical Communications Group 67 at Lincoln Laboratories, we have developed a new fiber optic OCDR system optimized for high speed and high detection sensitivity.[65] The device features a high speed translation device for fast data acquisition, optimized analog detection and signal processing electronics, and a modular probe which may be easily coupled to a slit-lamp biomicroscope. Low-coherence 830 nm light from a broad bandwidth superluminescent laser diode is launched into a fiber optic Michelson interferometer and split into reference and sample arms at a fiber coupler. Backscattered and retroreflected light from the biological sample is recombined with light returning from a scanning reference mirror. Coherent interference occurs at the detector only when the reference and sample arm optical path lengths match to within the source coherence length (17 μm FWHM). The reference mirror translates at a velocity of 38 mm/s which Doppler shift modulates the coherent interference signal at 93 kHz, a modulation frequency above the predominant optical and mechanical noise in the system. Detection and demodulation produce a profile of sample reflectivity versus depth. This heterodyne detection technique achieves quantum limited sensitivity and is able to resolve reflected signals as small as $\sim 10^{-10}$ of the incident optical power (> 90 dB dynamic range).

OCDR has many potential applications as a noninvasive medical diagnostic, especially in the transparent tissues of the eye. In collaboration with investigators at the New England Eye Center of Tufts University Medical Center and the Wellman Laboratories of Massachusetts General Hospital, we have examined medical applications which require the high-ranging resolution and high sensitivity possible with OCDR. We have used OCDR to demonstrate in vitro measurements of corneal thickness and excimer laser corneal excision depth, which are directly relevant to micron-precision monitoring of keratorefractive surgeries.[66] Our high speed OCDR system has allowed us to perform similar in vivo measurements in the anterior chamber of a rabbit eye, with no reduction in sen-

[64] R.C. Youngquist, S. Carr, and D.E.N. Davies, "Optical Coherence-domain Reflectometry: a New Optical Evaluation Technique," *Opt. Lett.* 12: 158 (1987); K. Takada, I. Yokohama, K. Chida, and J. Noda, "New Measurement System for Fault Location in Optical Waveguide Devices Based on an Interferometric Technique," *Appl. Opt.* 26: 1603 (1987).

[65] E.A. Swanson, D. Huang, M.R. Hee, J.G. Fujimoto, C.P. Lin, and C.A. Puliafito, "High-speed Optical Coherence Domain Reflectometry," *Opt. Lett.* 17: 151 (1992).

[66] D. Huang, J. Wang, C.P. Lin, C.A. Puliafito, and J.G. Fujimoto, "Micron-resolution Ranging of Cornea Anterior Chamber by Optical Reflectometry," *Lasers Surg. Med.* 11: 419 (1991).

sitivity or ranging resolution.[67] We have also found that OCDR has sufficient sensitivity to detail optical scattering within transparent structures such as the lens and cornea. Thus, OCDR is a potential clinical tool for the quantitative assessment of lens opacity and cataract progression. No objective technique for evaluating cataracts currently exists with sufficient reliability for routine clinical use. In preliminary studies, we have induced reversible "cold" cataracts[66] in enucleated bovine eyes and have investigated the correlation between the temperature dependent lens opacity and OCDR backscatter intensity.

We have also developed a birefringence sensitive OCDR system which can characterize the phase retardation of light reflected from different depths in biological tissue independent of probe orientation. Birefringence may be characteristic of particular tissue infrastructure due the directionality of fibrous nerve, muscular and connective tissue,[68] and may enhance contrast between different tissue structures when coupled with OCDR.

1.14.3 Optical Coherence Tomography

We have recently developed a new medical imaging technique called optical coherence tomography (OCT) which extends the ranging capabilities of single-axis OCDR and provides two-dimensional cross sectional images of optical reflectivity in tissue.[69] OCT functions in analogy to ultrasound B-mode imaging and measures cross sectional tomographic images by performing multiple longitudinal OCDR measurements taken at a series of lateral sample locations. A computer controlled stage translates the point of measurement a small lateral distance after each single longitudinal scan. The digitized scan sequences characterizing the tissue cross-section are mapped using image processing software to a gray-scale or false color image. Unlike x-ray computed tomography or magnetic resonance imaging, OCT does not require large amounts of computation for image reconstruction. As in the single scan case, the longitudinal resolution is determined by the source coherence length (17 μm FWHM), while the probe beam spot diameter determines the lateral resolution (9 μm FWHM). The optical sectioning capability of OCT is similar to confocal microscopy. Ranging resolution, however, is not limited by the available numerical aperture. Thus, OCT is useful for transpupillary imaging of the posterior eye and in endoscopic imaging.

In collaboration with the New England Eye Center and Wellman Laboratories, we have demonstrated OCT in a wide range of clinically relevant biological systems.[69] In vitro anterior eye tomographs provide comprehensive measurements of anterior chamber depth and corneal contour. These measurements address clinical problems such as narrow angle glaucoma diagnosis and fitting contact lenses. Backscattering from within transparent tissues such as cornea and lens is also clearly evident in these tomographs, which may also be clinically useful in assessing corneal opacity or cataract progression. OCT images of an in vitro retina in a resected eye show enhanced scattering from the retinal nerve fiber layer (RNFL) and retinal pigment epithelium. RNFL and total retinal thickness may be directly extracted from the image, suggesting a potential quantitative diagnostic tool for direct measurement of RNFL degeneration and open-angle glaucoma progression.[70] Currently, no quantitative method exists for the in situ evaluation of retinal nerve fiber loss. We have also examined OCT images in optically turbid media such as the artery. Tomographs of in vitro human coronary artery samples suggest that OCT can distinguish between the different scattering properties of fatty calcified arterial plaque versus fibro-usatheromatous plaque. Thus, a fiber optic OCT probe coupled to an endoscope might be potentially useful in distinguishing normal from diseased arterial walls in laser angioplasty surgeries.

---

[67] E.A. Swanson, D. Huang, M.R. Hee, J.G. Fujimoto, C.P. Lin, and C.A. Puliafito, "High-speed Optical Coherence Domain Reflectometry," *Opt. Lett.* 17: 151 (1992).

[68] R.N. Weinred, A.W. Dreher, A.C. Coleman, H. Quigley, B. Shaw, and K. Reiter, "Histopathologic Validation of Fourier-ellipsometry Measurements of Retinal Nerve Fiber Layer Thickness," *Arch. Opthalmol.* 108: 557 (1990).

[69] D. Huang, E.A. Swanson, C.P. Lin, J.S. Schuman, W.G. Stinson, W. Chang, M.R. Hee, T. Flotte, K. Gregory, C.A. Puliafito, and J.G. Fujimoto, "Optical Coherence Tomography," *Sci.* 254: 1178 (1991).

[70] H.A. Quigley and E.M Addicks, "Quantitative Studies of Retinal Nerve Fiber Layer Defects," *Arch. Opthalmol.* 100: 807 (1982).

1.15 Overview of the EUV Laser Effort

Professor Peter L. Hagelstein and his research group are very close to the commencement of experiments in search of gain at near 200 Å in low-Z or mid-Z nickel-like ions. The oscillator and pre-amplifier have been upgraded; the power amplifier is functional and awaits the completion of short pulse experiments; the target chamber is operational; some degree of target alignment capability is available; finally, two principal EUV spectral diagnostics have been installed and have taken data. These projects are described in the following sections. Plans for the near future include experiments at full power in search of gain at 191 Å in Ni-like molybdenum and similar studies in neighboring elements.

1.16 Nd:glass Amplifier Development

Sponsor

U.S. Department of Energy
Grant DE-FG02-89 ER14012-A003

Project Staff

Martin H. Muendel, Michele M. Bierbaum, Professor Peter L. Hagelstein

The upper laser state in the Mo laser at 191 Å is excited by 150-250 eV electrons; a 5-J, 10-GW laser beam is required to create a high-temperature plasma over a long cylindrical gain region. Such lasers are not readily available, and we have constructed a laser-amplifier system at 1.05 μm for driving the Mo-laser. The system consists of a zig-zag slab Nd:glass power amplifier which we have designed and constructed and a commercially available master oscillator and pre-amplifier. The various parts of the laser system are described below.

The oscillator is a standard active-modelocked, Q-switched Nd:YLF system generating 100 psec pulses at about 50 μJ. These pulses are apodized to give a supergaussian beam profile and are amplified to the 50 mJ level by an Nd:phosphate glass rod preamplifier operating in double pass.

A square apodizer and a vacuum spatial filter have been added following the preamplifier in order to produce a clean square beam profile. The apodizer works using a highly serrated aperture, with the low frequency spatial Fourier components corresponding to the required apodization. Passing the beam through the spatial filter results in removal of the high frequency modulation, and the resulting square beam exhibits a "top-hat" intensity profile with steep yet smoothly curved edges (to give the beam good propagation characteristics). A small vacuum system encompassing the region of the spatial filter pinhole is necessary in order to prevent atmospheric breakdown in the high intensity region near the laser focus; this system has been built and installed.

The beam is relayed by the spatial filter to the glass slab, which it traverses three times at a gain of 5× per pass to bring the total output energy to about 5 J. Two anamorphic prism pairs have been implemented to expand the beam to a rectangular cross section that matches the slab's clear aperture closely.

We have demonstrated energies in the 15-20 J range in 100 nsec pulses (non-modelocked); the damage limit for our system for such pulses is around 50 J. For modelocked, 100 psec pulses, we have been gradually bringing up the energy to the desired 5 J while watching for the onset of nonlinear self-focusing.

We have designed and fabricated an f/6 cylindrical lens doublet for the final focusing optic which is corrected for spherical aberration and coma and should be essentially diffraction-limited. The rectangular beam from the slab is thus imaged in one dimension to the target and tightly ($\tilde{1}0$ μm) focused in the other, which should result in a highly uniform line focus.

The slab amplifier's zig-zag rectangular geometry allows it to run at repetition rates over 0.5 Hz in spite of its quite large (20 cm^2) clear aperture. The limiting agent to the system's rep rate is the 1cm-diameter glass preamp rod, which has a thermal recovery time of 20-30 sec due to thermal lensing in the straight-through cylindrical geometry. We have purchased a large (0.8 cm diameter) Nd:YLF rod with which we intend to replace the glass rod. The crystalline YLF host has a tenfold higher thermal conductivity as well as lower thermal lensing than phophate glass, which should raise the preamp rep rate to over 0.5 Hz. Also, the sixfold higher gain cross section and lower nonlinear index of Nd:YLF make it a superior material for amplification of short pulses of very high peak power.

The combination of high output energy, high peak power and high repetition rate make this laser system unique. With the system at full output and, soon, at full rep rate, we expect it to serve as a powerful and flexible tool in our short wavelength gain studies.

1.17 Spectral Measurements of a Ni-like Mo Plasma

Sponsor

U.S. Department of Energy
Grant DE-FG02-89 ER14012-A003

Project Staff

Dr. Santanu Basu, James G. Goodberlet, Professor Peter L. Hagelstein

We are investigating gain at 191 Å between 4d and 4p levels in Mo XV in a laser produced plasma.[71] The condition for gain requires a temperature of around 200 eV and an electron density of 1.2×10^{19} cm^{-3} for production of MoXV ions, and excitation of the ground-state $3d^{10}$ electrons to the upper laser state. The upper laser state decays to 4f state by electron collisional excitation and to the lower laser level by radiation.

We have constructed two spectrometers for laser diagnostics: one is based on a Harada flat-field grating[72] and the other one uses a concave grating[73] with very little astigmatism. The spectra of Mo taken with the Harada grating spectrometer is shown in figure 3. The Mo spectrum was obtained using a train of 80-ps pulses, the energy per pulse being 7 mJ. The laser beam was focused with a f-15 spherical lens to a measured spot size of 41 μm, which produced 3.3×10^{12} W/cm^2 intensity on the target. This intensity level is comparable to the design intensity for the gain experiment. The spectrometer was calibrated using a carbon target and noting the positions of the following lines; C VI 1s-2p at 33.736 Å, C V 1s-3p at 40.268 Å, and 1s-2p at 40.268 Å. In the Mo spectrum, we noted the 3d-4p lines of Mo XVI at 46.86 Å, Mo XV at 50.44 Å, and MO XIV at 52.75 Å The results indicate that at the design intensity level for the gain experiment, Ni-like ions will be present in the plasma.

The streaked concave grating spectrometer (SCGS) uses a 32 x 30 mm concave grating of 1-m radius of curvature with 3600 lines per mm. The grating is used at near normal incidence which

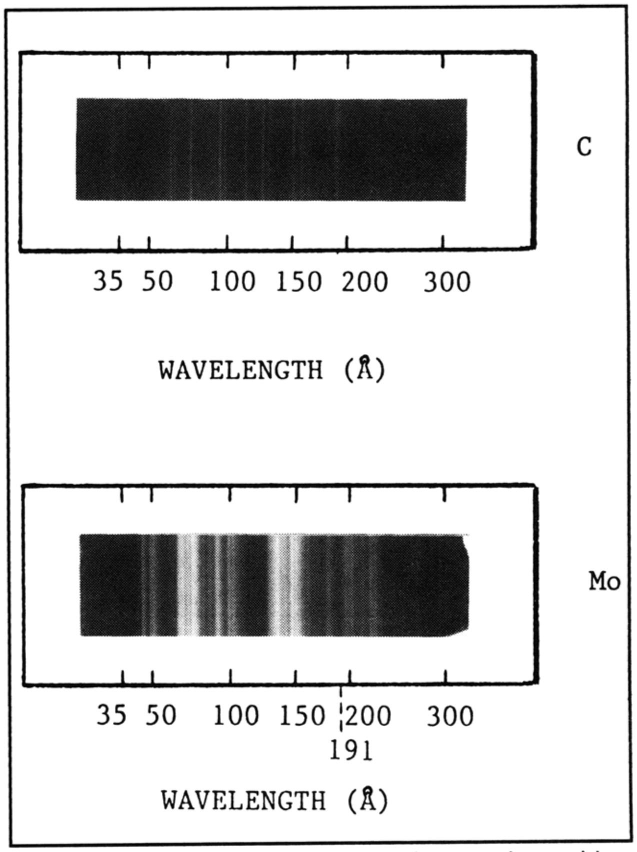

Figure 3. The spectrum of Mo plasma taken with a flat-field Harada grating spectrometer and an Al spectral filter. The spectrum of C was used for calibration.

produces a nearly stigmatic image, at the cost of negligible reflectivity at less than approximately 180 Å. The image magnification is 2.2, and the minimum astigmatic blur is estimated to be only 663 μm, which will make the SCGS a valuable diagnostic tool for time resolved and spectrally resolved imaging of the plasma. A streak camera with 12.5-mm wide photocathode is used to obtain temporal information on the x-ray spectrum over a 22 Å range.

Calibration for this spectrometer was carried out with Al as target material and at an incident intensity of $2 - 5 \times 10^{12}$ W/cm^2. Polaroid 107 which has a dynamic range of only 100 was used to record the spectrum in our first experiment. The

[71] P.L. Hagelstein, S. Basu, M.H. Muendel, J.P. Braud, D. Tauber, S. Kaushik, J. Goodberlet, T.-Y. Hung, and S. Maxon, "The MIT Short-Wavelength Laser Project: A Status Report," *Proceedings of the International Colloquium on X-Ray Lasers,* York, United Kingdom, 1990, p. 255; S. Basu, M. Muendel, J. Goodberlet, S. Kaushik, and P.L. Hagelstein, "A Search for Gain at 191 Å," *Proceedings SPIE International Symposium on Optical Applied Science and Engineering,* San Diego, California, July 1991.

[72] T. Kita, T. Harada, N. Nakano, and H. Kuroda, *Appl. Opt.* 22(4): 512 (1983).

[73] U. Feldman, G.A. Doschek, D.K. Prinz, and D.J. Nagel, *J. Appl. Phys.* 47(4): 1341 (1976).

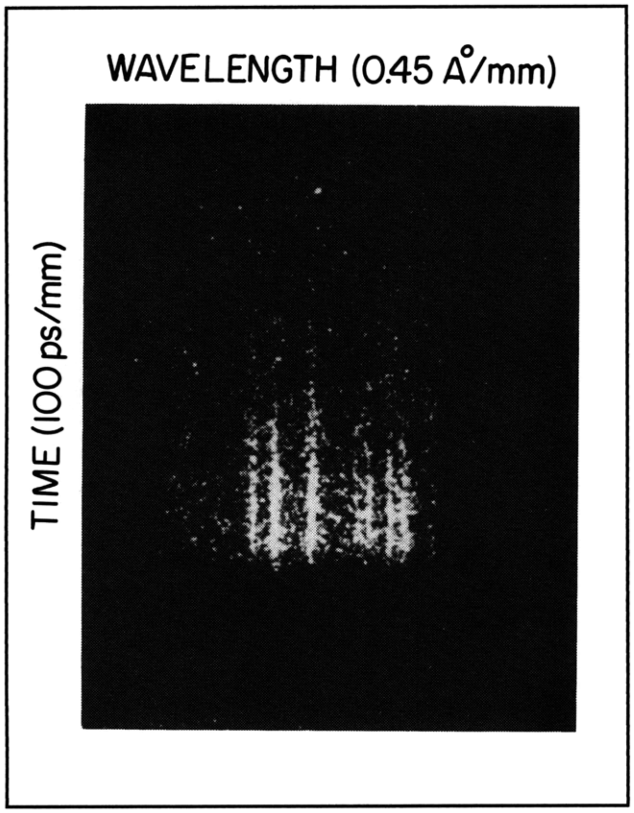

Figure 4. Calibration of the streaked concave grating spectrometer (SCGS). The spectral lines shown in this photograph are (from left to right): Al VII, 239.03 Å, Al VII, 240.77 Å, Al VI, 243.77 Å, Al VIII, 247.35 Å, 0 V, 248.46 Å, Al VIII, 250.14 Å, Al VIII, 251.35 Å,

data is shown in figure 4. The bright line at the center of the photograph is the Al VI line at 243.766 Å. The two lines on the extreme right at 250.139 Å (Al VII) and 251.347 Å (Al VIII) are separated by 1.21 Å and are clearly resolved. The spectral resolution at 240 Å was estimated to be 0.6Å($\lambda/\Delta\lambda = 400$). The SCGS also allows us to look at the x-ray spectrum over a number of pump pulses which are separated by 7.5 ns.

In our design, both the spectrometers are installed inside of the chamber. The design has proved to be very efficient, since it is compact and it minimizes the impact of external vibrations on the diagnostic system. We envision the x-ray laser system to be operated routinely by one person in a university setting. Except for the externally applied pump beam, the completely enclosed x-ray laser head functions not much differently from commercially available optical laser heads. We have diagnosed laser produced plasma using a flat-field spectrometer, and a streaked concave grating spectrometer and these instruments are now ready to measure gain down to a gain-length product of 1.

1.18 Progress in EUV Laser Kinetics Modeling

Sponsor

U.S. Department of Energy
Grant DE-FG02-89 ER14012-A003

Project Staff

Professor Peter L. Hagelstein

The analysis of laser kinetics for x-ray lasers historically has relied extensively on large numerical simulation models which use several hundred levels to model the population dynamics. We have recently succeeded in developing an effective three-level model which accurately reproduces the temperature and density dependence of the population dynamics of the upper and lower laser states in mid-Z nickel-like ions obtained from the large models.

We have found[74] that the fractional inversion density is well approximated by

$$\frac{N^*}{N_o} = \frac{C_{uo}}{C_u}\left[\frac{x}{1+x} - \zeta\frac{x}{(1+x)^{1/3}}\right]$$

where N^* is the inversion density on the $3d^94d^1S - 3d^94p^1P$ laser transition, and N_0 is the ground state $3d^{10}$ population. The collisional rate up to the laser state is C_{uo}, and the collisional destruction rate of the upper laser state is C_u. The parameter x is the electron density normalized to the upper state equilibration density

$$x = \frac{C_u}{A_u}$$

where A_u is the radiative decay rate of the upper laser state. The parameter ζ describes the efficiency with which the ground state is populated, and evaluates to

$$\zeta = \frac{1}{3}\frac{A_u}{A_l}\frac{C^*_{lo}}{C_{uo}}$$

[74] P.L. Hagelstein, "Development of the MIT Short Wavelength Laser," *Proceedings SPIE International Symposium on Optical Applied Science and Engineering,* San Diego, California, July 1991.

In this formula, A_l is the radiative decay rate of the lower state, and C^{*}_{lo} is the total collisional rate up to the lower laser state which would be obtained by taking the zero-density limit of the excitation cross section for all direct and indirect processes.

This result has allowed us to optimize analytically the optimum plasma temperature and electron density for maximum gain for mid-Z nickel-like ions. The optimum temperature occurs near $kT_e = \Delta E/2$, where ΔE is the excitation energy to the upper state. The optimum density occurs near

$$x \approx \left[\frac{3}{5\zeta} \right]^{3/2}$$

valid to within about 20% in regimes of interest.

We have verified independently that our proposed operating point for Ni-like Mo is in fact optimum, and have found scaling relations for neighboring elements. Interestingly enough, scaling to low Z appears to be problematic in Ni-like ions using a 1 μ driver, due to the very low density (and hence low gain) which occurs under optimum plasma conditions.

1.19 Laser Cavities in the Soft X-Ray Region

Sponsor

U.S. Department of Energy
Grant DE-FG02-89 ER14012-A003

Project Staff

John Paul Braud, Professor Peter L. Hagelstein, Dr. Santanu Basu, Tsen-Yu Hung

The primary motivation in developing laser cavities is to make a significant improvement in the beam quality and efficiency of extraction of stored energy in the gain medium. We have been working on whispering-gallery optics for short-wavelength laser cavities.[75]

We have made a major step forward in the analysis of beam propagation in whispering-gallery mirrors (WGMs). Our previous work in this area had led to the development of what we called the "whispering-gallery equation," which describes the evolution of a beam's transverse structure as it propagates along the surface of a WGM. During the past year, we have managed to solve this equation analytically; the solutions that we found are quasi-adiabatic local normal modes having curved wavefronts.

This progress in the area of analysis has in turn clarified the problem of design. Since the beginning of this project, an important goal has been the development of elongated mirror shapes leading to reduced beam divergence relative to the more obvious circular design. In the past year, we discovered a new class of mirror shapes, the so-called "quadratic family," whose performance in this regard is vastly superior to any designs considered previously. The primary virtue of a rotationally symmetric design is the relative ease of manufacture.

We have also made progress in establishing surface finish requirements for WGMs. We have developed a coupled-mode approach to describe the effect of surface imperfections and thereby established fabrication tolerances. The finish requirements for WGMs were found to be qualitatively different from those appropriate to more conventional optics.

We are also continuing to explore the use of unstable resonators. The high gain and short lifetime typical of short-wavelength laser amplifiers match up ideally with the large output coupling and rapid spatial-mode formation characteristic of unstable resonators. Moreover, unstable resonators can rely on diffractive output coupling and thereby avoid the use of beamsplitters, which are enormously inefficient at short wavelengths. The design of an unstable resonator with readily avail-

[75] T.-Yu Hung and P.L. Hagelstein, "Whisper Gallery Mirrors Reflectivities from 100 Å to 500 Å," *Proceedings of the International Conference on Lasers 90,* San Diego, California, 1990; T.-Yu Hung and P.L. Hagelstein, "Investigations of Whisper Gallery Mirrors for Extreme Ultraviolet (EUV) and Soft X-rays," *IEEE J. Quant. Electron.* (1992), forthcoming; J.P. Braud and P.L. Hagelstein, "Whispering-Gallery Laser Resonators—Part I: Diffraction of Whispering Gallery Modes," *IEEE J. Quant. Electron.* 27: 1069 (1991); J.P. Braud and P.L. Hagelstein, "Whispering-Gallery Laser Resonators—Part II: Analysis of Mirrors with Non-Uniform Curvature," *IEEE J. Quant. Electron.* 28: 254 (1992); J.P. Braud and P.L. Hagelstein, "Whispering-Gallery Laser Resonators—Part III: Mirror Design," submitted to *IEEE J. Quant. Electron.* (1992); J.P. Braud, "Polarizing Optics for the Soft X-ray Regime: Whispering-Gallery Mirrors and Multilayer Beamsplitters," *Proceedings of the SPIE International Symposium on Optical Applied Science and Engineering,* San Diego, California, July 1991; J.P. Braud, "Whispering-gallery Mirrors for Short-wavelength Laser Cavities: Shapes and Tolerances," *Proceedings of the SPIE International Symposium on Optical Applied Science and Engineering,* San Diego, California, July 1991.

able multilayer optics for our laser system is included in Basu and Hagelstein.[76]

1.20 Boltzmann Equation Studies

Sponsor

U.S. Department of Energy
Grant DE-FG02-89 ER14012-A003

Project Staff

Ann W. Morgenthaler, Professor Peter L. Hagelstein

A necessary step in the development of an x-ray laser is characterization of the collisionally-excited plasma produced by bombarding a high atomic number substrate with an intense electromagnetic field. If the density, velocity, and temperature profiles of the plasma are known, it is then possible to compute the expected laser gain directly. Much progress has been made in numerically simulating the hydrodynamics of x-ray laser plasmas, but usual assumptions of local thermal equilibrium are often insufficient to accurately calculate thermal conductivities, plasma viscosities, etc. As part of an attempt to produce a table-top x-ray/EUV laser, we are developing one- and two-dimensional hydrodynamics codes which will describe the behavior of non-Maxwellian coronal plasmas in the free-streaming limit where the linearized transport coefficients are typically inaccurate.

A general solution to the collisional Boltzmann equation is proposed, which consists of taking velocity moments of the scalar distribution function f(x, v; t). The velocity dependence thus disappears from the Boltzmann equation at the expense of solving an infinite number of coupled moment equations. It is our hope that only a few of these moment equations will be necessary to determine the behavior of the first three (namely, density, velocity, and temperature). If we define **h**, an infinite-dimensional column vector with components

$$h^{abc}(x, t) \equiv N < u_x^a u_y^b u_z^c > = \int d^3u \; u_x^a u_y^b u_z^c f(x, u; t) \qquad (1)$$

where N is the plasma density, $u = v - <v>$ is the fluctuation velocity and a, b, and c take on the values of all non-negative integers, it is straightforward to show that the vectorized Boltzmann equation is:

$$Dh = h \bullet C \bullet h \qquad (2a)$$

$$D = \frac{D}{Dt} + (\nabla \bullet <v>) + \qquad (2b)$$

$$\left(\left(\frac{D<v>}{Dt}\right) - a\right) \bullet L^- + \nabla \bullet L^+ + L^+ \bullet (\nabla <v>)L^-$$

where $D/Dt = \partial/\partial t + <v> \bullet \nabla$ is the usual convective derivative and the raising and lowering operators L^+ and L^- are defined in component form as:

$$\begin{aligned} L_x^-\Phi^{abc} &= a\Phi^{a-1bc} & L_x^+\Phi^{abc} &= \Phi^{a+1bc} \\ L_y^-\Phi^{abc} &= b\Phi^{ab-1c} & L_y^+\Phi^{abc} &= \Phi^{ab+1c} \\ L_z^-\Phi^{abc} &= c\Phi^{abc-1} & L_z^+\Phi^{abc} &= \Phi^{abc+1} \end{aligned} \qquad (3)$$

where Φ^{abc} is any function indexed by the non-negative integers a, b, and c.

We have calculated exact formulas for the three-dyad *C* based on expanding the distribution function f in the eigenmodes of the spherical harmonic oscillator $\{|nlm>\}$ with the indices $n, l \in [0, n]$, $m \in [-l, l]$ analogous to the quantum numbers in the spherical harmonic oscillator problem. These functions (also called the Burnett basis) are products of spherical harmonics and associated Laguerre polynomials, with $|000>$ representing the local, shifted Maxwellian distribution. The full, non-linear Boltzmann equation may then be solved numerically for an arbitrarily anisotropic distribution, though clearly more moment equations will be needed if the distribution is severely non-Maxwellian.

The nonlinear problem is often linearized by assuming that one of the collision partners (represented by either h on the right side of equation 2a) is Maxwellian, and we can use our formulation to compute the linearized transport coefficients directly from the vectorized Boltzmann equation. The transport equations are found from a matrix equation having the form:

$$\sum_{n=0}^{\infty} J_{kn}A_n = b_k \qquad k = 0,1,2,... \qquad (4)$$

where J is related to the linear collision matrix and b is also known; the transport coefficients are

[76] S. Basu and P.L. Hagelstein, "Design Analysis of a Short Wavelength Laser in an Unstable Resonator Cavity," *J. Appl. Phys.* 69(4): 15 (1991).

functions A_0 in this schematic description. Clearly, the first approximation to A_0 is just b_0/J_{00} and more sophisticated estimates can be made by truncating n at larger values. The Chapman-Enskog and Réisibois formulations only find the first approximation of the transport coefficients (and our formulation agrees exactly with their results). By vectorizing the Boltzmann equation and calculating the collision cross-sections exactly, it is easily possible to find the higher-order estimations of the transport coefficients. The thermal conductivity κ is typically approximated as

$$\kappa = \frac{75}{32\sqrt{\pi}} \frac{k(kT)^{5/2}}{e^4 m^{1/2} \ln \Lambda} \tag{5}$$

which is also our first order result, and we can show that this linear conductivity is typically 20% too low. The transport coefficients converge rapidly as more terms in (4) are used, with 99% accuracy if n is truncated after n=4.

The next phase in this research will be to implement the non-linear equations in one- and two-dimensional form, since the laser plasma is not well described by the linear model. Adaptive Lagrangian codes with Newton-Raphson solvers will probably be the methods of choice.

1.21 Coherent Fusion Studies

Project Staff

Professor Peter L. Hagelstein, Isaac L. Chuang, Sumanth Kaushik, Irfan U. Chaudhary

The past year has seen advances in many areas of cold fusion research, and, in addition, a number of new effects have recently been reported. In this article, we will summarize briefly the current status of the field and review theoretical progress which we have made during the past year.

The primary effect associated with cold fusion research is the production of excess heat in electrochemistry experiments. During the past year, Pons and Fleischmann reported[77] obtaining completely reproducible heat excesses in the 20-50% regime, and described rather dramatic events where the excess power would be on the order of 10 times the input electrochemical power for periods of roughly half an hour. These high power events had been seen on eleven occasions as of the July meeting in Como, Italy; the new experiments benefited from the use of rods made of $Pd_{0.9}Ag_{0.1}$.

Reproducible heat was also reported by McKubre at SRI,[78] who described a recipe which had been discovered which produced excess heat on every occasion which the conditions of the recipe had been met. In total, the observation of about 100 bursts of excess heat was reported; these bursts occured during ten multimonth runs. Heat excesses of 10-20% were seen many times, measured with an accuracy of a few tenths of a per cent.

Heat in light water experiments has recently been reported by Mills and coworkers,[79] a result which is being viewed with skepticism by those who have observed heat in heavy water Pons-Fleischmann experiments. While still preliminary in that confirmations of the result have not yet been reported, the experimental claim is the generation of about a factor of 2 excess heat using nickel cathodes and a potassium carbonate electrolyte with very low current density ($\sim$ mA/cm^2), rather than using palladium cathodes and a LiOD electrolyte. This result is potentially important for numerous reasons: (1) Ni and light water are cheaper than Pd and heavy water, and (2) if correct, the result has the potential to demolish several classes of proposed mechanisms.

Very significant levels of ^{4}He have been reported from heat-producing Pons Fleischmann experiments.[80] The ^{4}He appears to be a byproduct of the heat process, but cannot quantitatively account for the heat produced.

Slow tritium production has been controversial since tritium contamination was claimed close to two years ago. Since that time, a number of groups have set up experiments in which tritium production is observed at the same time that pos-

77 M. Fleischmann, presented at the Second Annual Cold Fusion Conference, Como, Italy, July 1991.

78 M. McKubre, R. Rocha-Filho, S. Smedley, F. Tanzella, S. Crouch-Baker, T. Passell, and J. Santucci, "Isothermal Flow Calorimetric Investigations of the D/Pd System," *Proceedings of the Second Annual Cold Fusion Conference*, Como, Italy, July 1991.

79 R. Mills and S. Kneizys, *Fusion Tech.* 20: 74-81 (1991).

80 B.F. Bush, J.J. Lagowski, M.H. Miles, and G.S. Ostrom, "Helium Production During the Electrolysis of D_2O in Cold Fusion Experiments," *J. Electroanal. Chem.*, forthcoming.

sible metal contamination is assayed. Will et al. reported reproducible tritium production in palladium electrolysis using deuterated sulfuric acid;[81] Lanza described tritium production in a number of host alloys at similar levels;[82] Claytor reported tritium from his gas phase work.[83] Extremely high levels of tritium production have been claimed recently by Chien in electrolysis experiments.[84]

Observations of fast particle production are still being reported, with studies making some progress towards the determination of particle charge, mass and energy. Work on neutrons is continuing. Fleischmann recently described neutron observations from recent experiments of his group in a talk at MIT last December, in part to respond to the errors found in their initial neutron measurements.

We have been continuing our efforts to develop a theory which would apply to the Pons-Fleischmann effect and related anomalies which have been reported.[85] The premise of our current model is that energy transfer between nuclei and a lattice may occur through what amounts to a recoil effect, described by an interaction Hamiltonian of the form

$$\hat{H} = \int \hat{\Psi}_f[-\mu \bullet \hat{B}]\hat{\Psi}_i \wedge \hat{\psi}_n + \text{H.c.}$$

for magnetic dipole mediated neutron transfers, where the field operators describing nucleons in the lattice are of the form

$$\hat{\Psi}_i(\{r\}) = \sum_j \Phi_i(\{r - \hat{R}_j\})\hat{b}_i(j)$$

and where $\hat{R}_j$ is the lattice operator describing the center of mass of a nucleus at site j. This interaction Hamiltonian provides a natural description of recoil effects associated with neutron capture on a nucleus which is embedded in a lattice. This hamiltonian can be used to obtain lineshapes for direct conventional neutron capture in a lattice.

The transfer of a nuclear quantum of energy to lattice phonons in this theory requires a very high nonlinearity, which is provided naturally through the recoil effects contained in the interaction hamiltonian given above. The essential physics of the transfer is contained in the hamiltonian resulting from averaging over all coordinates except for phonon coordinates

$$\hat{H} = \sum_m \hbar\omega_m \hat{a}_m^\dagger \hat{a}_m + [V(t)e^{-i\hat{S}} + \text{H.c.}]$$

where V(t) is a high frequency (MeV) signal from the nuclear states, and where $e^{-i\hat{S}}$ is a Duschinsky operator which scales and translates according to

$$e^{-i\hat{S}}\Psi_L(q) = C\Psi_L(A \bullet q + b)$$

This operator takes into account the fact that the lattice differs before and after the capture process.

Energy transfer may occur if the high frequency nuclear signal can be demodulated. If a multimode phonon state is constructed from a product of single mode states,

$$\Psi_L = \prod_m \psi_m(q_m, t)$$

then self-consistent hamiltonians for each individual mode can be obtained of the form

$$\hat{H}_m = \hbar\omega_m \hat{a}^\dagger \hat{a} + V(t) < e^{-i\hat{S}} >_{\overline{m}}$$

If a very large number of modes can be locked, then the self-consistent single mode potential $V(t) < e^{-i\hat{S}} >_{\overline{m}}$ can be demodulated to have a low

[81] F. Will, K. Cedzynska, M-C Yang, J.R. Peterson, H.E. Bergeson, S.C. Barrowes, W.J. West, and D.C. Linton, "Studies of Electrolytic and Gas Phase Loading of Palladium with Deuterium," *Proceedings of the Second Annual Cold Fusion Conference,* Como, Italy, July 1991, p. 373.

[82] F. Lanza, presented at the Second Annual Cold Fusion Conference, Como, Italy, July 1991.

[83] T. Claytor and F. Lanza, presented at the Second Annual Cold Fusion Conference, Como, Italy, July 1991.

[84] C. Chien and T.C. Huang, "Tritium Production by Electrolysis of Heavy Water," unpublished, 1991.

[85] P.L. Hagelstein, "Coherent and Semi-Coherent Neutron Transfer Reactions I: The Interaction Hamiltonian," *J. Fusion Tech.* (1992), forthcoming; P.L. Hagelstein, "Coherent and Semi-Coherent Neutron Transfer Reactions II: Dipole Potential Operators," submitted to *J. Fusion Tech.*; P.L. Hagelstein, "Coherent and Semi-Coherent Neutron Transfer Reaction Mechanisms," submitted to *J. Fusion Tech.*

frequency component. To lowest order in the single mode potential, coherent states will be generated; to higher order, squeezed states are generated. Future efforts will focus on the relative contributions of each effect.

This model appears to have the potential to lead to the basic effect, and results in mean-field mode equations which may be be solved self-consistently.

The theory leads to a donor and acceptor nucleus description of coherent neutron transfer reactions (see figure 5). Heat in Pons-Fleischmann experiments is proposed to be due to the transfer of neutrons from deuterons to ^{6}Li nuclei; tritium comes about from neutron transfer to deuterons; ^{4}He and a high energy beta is evolved following neutron capture on ^{7}Li The light water experiments could be accounted for by neutron transfers on ^{39}K.

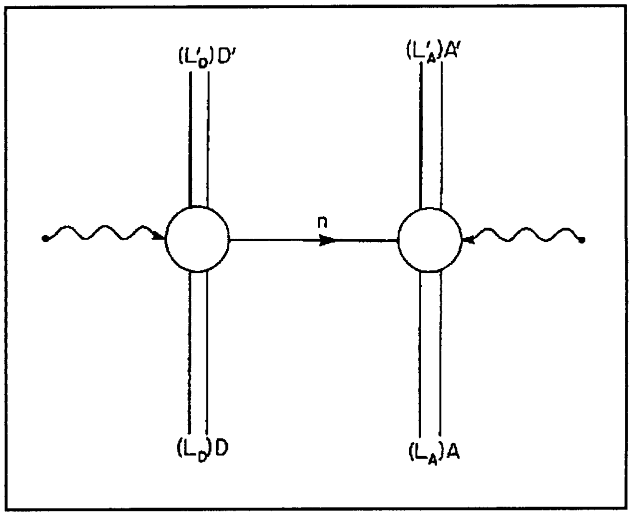

Figure 5. A general two-step coherent neutron transfer reaction for heat production. D and A refer to donor and acceptor nuclei before the transfer and primed variables refer to post-transfer variables. L_D and L_A refer to the host lattice.

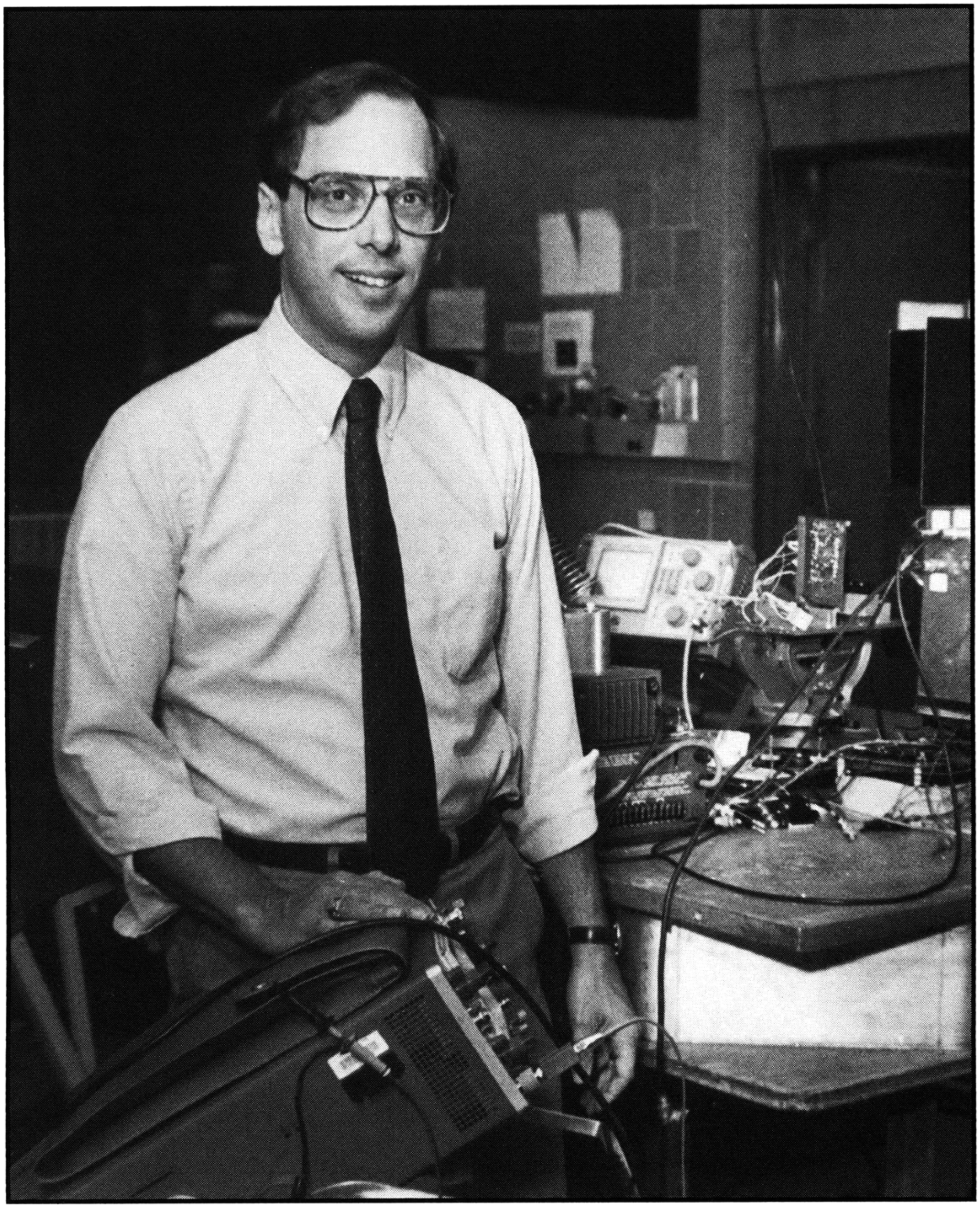

Professor Jeffrey H. Shapiro